On the properties of magnetic pulsations in the solar wind

Anders Ericsson

On the properties of magnetic pulsations in the solar wind

Anders Ericsson

Master of Science Thesis in
Physical Electrotechnology

Stockholm, March 2005

On the properties of magnetic pulsations in the solar wind

Anders Ericsson

Division of Plasma Physics (Space Plasma Group), Alfvén Laboratory
Royal Institute of Technology, SE-100 44 STOCKHOLM, SWEDEN

Abstract

An investigation of certain properties of the magnetic field pulsations in the solar wind has been conducted. Power spectra of 6 hour time series of the magnetic field magnitude in the solar wind at 1 AU was examined for the time period of 1997-2004. Focus lied on power spectra that showed one or two clear peaks characterizing simple wave phenomena of varying duration. The frequency distributions of these peaks were observed using two frequency spans in the Pc-5 region. The mean angle of the total magnetic field during these periods were examined and the spectra of the magnetic field components were compared to the spectra of the magnetic field magnitude. In addition, the occurrence distribution of the events during 1997-2004 were examined for long-term variations. It was found that no wave phenomena with a particular frequency or mean angle was predominant in the events in this study. The direction of the total magnetic field during these events were consistent with the mean direction calculated over a long time. Variations related to the events in the study were found to exist at periods of 11 years, 1.4 years, 0.3 years and 29 days. The duration of the pulsations seen were in all cases shorter than 6 hours. Many of the pulsations were of shorter duration lasting only an hour or two or even a fraction of an hour.

Sammanfattning

En studie av vissa egenskaper hos pulsationer i det magnetiska fältet i solvinden har genomförts. Effektspektra av 6-timmarsperioder av magnituden av det magnetiska fältet vid 1 AU undersöktes för tidsperioden 1997-2004. Fokus har legat på effektspektra som visar en eller två tydliga spektraltoppar vilket indikerar ett enkelt vågfenomen med varierande varaktighet. Frekvensfördelningen för dessa spektraltoppar observerades för två frekvensspann i Pc-5 området. Det totala magnetfältets vinkel undersöktes och magnetfältkomponenternas spektra jämfördes med spektra för magnituden av magnetfältet. Tiden då dessa händelser inträffade undersöktes också för perioden 1997-2004. Resultaten visar att ingen frekvens är mer förekommande än andra i de två undersökta frekvensområdena. Riktningen av magnetfältet var i överensstämmelse med medelvärdet beräknat under lång tid. Vidare visar resultaten att det existerar variationer med periodtider på 11 år, 1.4 år, 0.3 år och 29 dagar. Varaktigheten för de observerade pulsationerna är för det mesta kortare än sex timmar. Många pulsationer uppvisar ett kortare förlopp och varar bara en timme eller två eller till och med bara bråkdelar av en timme.

Contents

1 Introduction

The solar wind is an area of intense scientific study and has been since the launch of the first research satellites in the 1960s, but discussions occurred even long before that at times where in-situ measurements were merely a dream. The early science was, due to the lack of empirical evidence, quite theoretical and mainly involved with terrestrial magnetospheric observations and was full of speculative and imaginary ideas. Many mathematical concepts were not yet developed and scientific papers were mainly written on the foundation of the writers insight for the subject and their creative minds. But considering the sparse information that scientists relied on at this time it is interesting to see that many fundamental ideas of magnetospheric physics today were glimpsed during those early years. Though many ideas and notions have resulted in consensus over the years many aspects of the solar wind remain a conundrum considering the many fields of physics involved. Still, many basic questions that are unanswered exist.

One of those questions is related to the characteristics of the fluctuations seen in the solar wind parameters. The fluctuations can be observed in all of the solar wind variables and the main focus of this work is disturbances in the magnetic field. The nature of these fluctuations have been investigated since the very beginning of the space age but the complete picture has not yet been drawn. It is assumed that most of the fluctuations are transverse to the mean magnetic field and that the distinction between waves and turbulence (wave phenomena of very short duration) is dim. Since the solar wind interacts with the magnetosphere, and it has been observed that wave phenomena occur inside of it, it has been suggested that some of these magnetospheric pulsations are directly linked to pulsations of the same frequency in the solar wind. Therefore, a statistical analysis of the frequencies of the disturbances in the solar wind magnetic field has been conducted in this work. The work is based on the legitimacy of a simple power spectral technique to accurately distinguish periods where few (one or two) spectral peaks can be seen and to relate those peaks to a real physical event in the magnetic field.

The first indication of an interaction between the Earth and the Sun was in 1852 when the British scientist Sabine discovered a positive correlation between the number of sunspots and magnetic storms [20]. It was at this time the German pharmacist and hobby astronomer Schwabe got his discovery published in the third volume of Alexander von Humboltz's Kosmos and the information about the sunspot number became available to the scientific community for the first time. As early as 1741 Celsius reported a positive correlation between the events auroras and magnetic storms but no information was available to him to notice the relationship with the sunspot number. At the time of Schwabes tables of sunspot numbers the correlation between the aurora and the sunspot number was soon found as well. Although the connection existed no one could understand the coupling between the Sun and the Earth. Eight years later Carrington and Hodgson independently noticed a bright, sudden light emerging from the Sun when examining sunspots and a large magnetic storm 17 hours

later [3]. Something was travelling from the Sun to the Earth faster than 1000 km/s but no one at this time knew what it was.

Laboratory tests made by Birkeland on charged particles and spherical magnets in vacuum in the beginning of the twentieth century and the quite well documented aurora led to the conclusion that it was a stream of charged particles (electrons, although the exact particle species was not known at the time) that was streaming out of the Sun. At the time of arrival at Earth the particles are then guided along the Earth's magnetic field lines down to the poles. The current also led to the creation of a magnetic field which explained the disturbance in the magnetic field at Earth. The problem with a stream of electrons was that it would quickly disperse due to the repelling electrostatic force between the electrons. This problem was solved with the new notion of a neutral cloud of electrons and ions (a plasma) being the building blocks of the stream [26].

Since the era of space flight the parameters that characterize the solar wind have been thoroughly investigated. The measured volume in space extend from near the Sun at 0.3 AU to the edge of the heliosphere at more than 100 AU [11][8][6]. A manifold of experiments have imaged the solar wind in time scales of years to fractions of seconds. Despite the large amount of information collected over the years there are features in the solar wind that are unexplained. The fluctuations seen in the magnetic field, density, velocity, temperature and other variables are not fully understood and the search for the origin of these fluctuations, and understanding the dynamics of them, is a driving force of this research area.

2 Basic space physics

Magnetospheric and solar wind physics deal with a wide variety of plasma populations each with properties that are somewhat different from the others. In this chapter a description of the magnetosphere and the solar wind, and the physics related to these regions, are made. First, the magnetosphere is described and then the physics behind the MHD theory and the associated MHD waves are depicted. Several types of the perturbations seen in solar wind variables are based on this theory.

2.1 The solar wind

The solar wind is a high-speed particle stream flowing from the Sun with a mean velocity of about 500 km/s. Streams with velocities below this value are called slow solar wind streams and streams with velocities above it are called fast solar wind streams. However, velocities over 1400 km/s have been shown to exist for shorter periods but also events where the velocity was extremely low have been observed [23][22][14]. The solar wind expands and fills interplanetary space where it interacts with the magnetic fields of the planets and causes magnetic storms and auroras. The volume in space where the solar wind exists is called the heliosphere. How far out it reaches is unknown but estimations show that it at least reaches 100 AU (1 AU is the mean distance between the Sun and the Earth) and recently Krimigis et al. showed that the heliosphere extends to at least 85 AU [11].

The fast solar wind is believed to have its origin in coronal holes where the magnetic field lines are open and unable to obstruct the outflow of plasma. These areas are therefore somewhat colder than the areas around the holes and the absence of closed magnetic field lines also gives the plasma a somewhat higher radial velocity than from other areas. The slow solar wind is believed to come from streamers originating from areas where the field lines are not completely closed making it possible for some of the solar material to escape the Suns gravity but at a lower speed than that of the fast solar wind. Since the Sun's photosphere is too cold to accelerate the solar wind to its high velocity the corona is believed to be the source for the supersonic and superalfvènic velocities observed.

The solar wind is a thin, fully ionized plasma (at least at 1 AU) consisting mostly of protons, electrons and alpha particles. Ionized helium and alpha particles typically account for 1-5 % but occasionally as much as 10 %. Several other heavier ions also contribute to the particle composition but the densities of these particles are very low compared with that of protons, roughly 1 % in total of the number density. Of the heavier particles involved, different ionized oxygen and iron make up the more dominant part [9]. Typical values of solar wind variables are listed in Table 1 below. Since the solar wind is a plasma the criterion for quasi-neutrality is fulfilled and on sufficiently large spatial scales the electron number density are equal to the sum of the proton and alpha-particle number density. Of course, the heavier ions also contribute to the quasi-neutrality but their occurrence is low so they can often be neglected.

The Sun rotates with a period of 27 days and the magnetic field of the Sun is drawn out into a spiral shape known as the Archimedes spiral. The solar wind is therefore not radial but rather makes an angle in the ecliptic plane which at

Parameter	Typical Value
Bulk speed	450 km/s
Proton density	$6.6 \ cm^{-3}$
Helium density	$0.1\text{-}0.3 \ cm^{-3}$
$|\mathbf{B}|$	6 nT

Table 1: Typical values of different solar wind parameters

1 AU is about 45 degrees to the Sun-Earth line. The meridional angle is small compared to the angle in the ecliptic plane. Both angles vary with time.

In a vacuum the magnetic field from a dipole rapidly vanishes and no solar magnetic field would therefore exist at Earth but would rather be confined to the vicinity of the Sun. This magnetic carrying property of the solar wind is the effect of frozen-in magnetic field lines. The concept of frozen-in field lines was introduced by Alfvén in 1940 [5], and occurs when the plasma is highly conductive. When the ratio of magnetic to kinetic energy density is low the plasma motion drags the magnetic field along (if the ratio is high, the plasma motion is controlled by the magnetic field).

2.2 The magnetosphere

The inherent magnetic field of the Earth creates, in the vicinity of the planet, a cavity in space called the magnetosphere. Inside the *magnetosphere* the physical processes and ranges of many quantities are different compared to those outside the cavity. The outer rim of the magnetosphere is called the *magnetopause* and defines the boundary of this region. Towards the Sun the magnetosphere is compressed by the solar wind and the extent of the magnetosphere towards the Sun is therefore much smaller than on the night side where it is drawn out into a *magnetotail*. Many different plasma populations exist inside the magnetosphere and the physical properties and processes vary considerable between these populations.

2.2.1 The structure of the magnetosphere

As mentioned earlier the magnetopause is the outer boundary of the magnetosphere. However, the very first interaction between the terrestrial magnetic field and the solar wind occurs even further towards the Sun at the *bow shock*. The bow shock is a shock front analogous to that of the bow shock in front of a supersonic airplane. It exists because the terrestrial magnetic field acts as an obstacle to the supersonic solar wind. The bow shock are further discussed in Section 2.2.2. Outside the bow shock the solar wind is both supersonic and superalfvénic and inside it is subsonic and subalfvénic. The region between the magnetopause and the bow shock, occupied by a subsonic flow of solar wind plasma, is called the *magnetosheath* and is about 2 or 3 R_E (R_E is one Earth radius) thick. Plasma in the magnetosheath shows strong turbulence and a magnetic field that is weaker than that inside the magnetopause. Figure 1 shows the magnetosphere with its different plasma populations and currents.
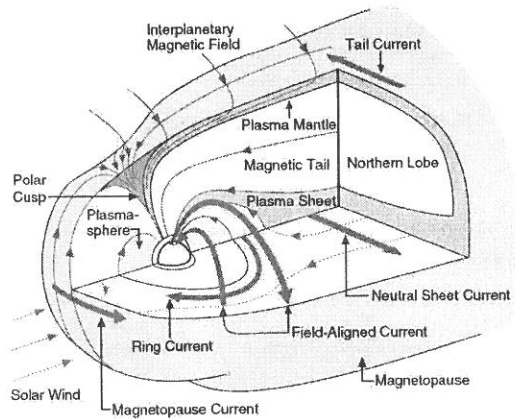
Figure 1: The magnetosphere. (From *The Solar Wind Interaction with the Earths Magnetosphere: A Tutorial*, Russel, C. T.)

In the ecliptic plane towards the Sun the magnetopause boundary show no irregularities and on the sides of the planet it is smoothly drawn out towards the tail. However, looking in the meridional plane the terrestrial dipole magnetic field changes topology from day-side like to night-side like creating neutral points at the magnetic poles. These are the *polar cusps* and are the main entry points of the solar wind into the magnetosphere. The polar cusps are directly connected to the ionosphere.

The *plasmasphere* is a continuation of the ionosphere at mid and low latitudes and is a torus-shaped volume filled with cool and dense plasma originating from the underlying ionosphere. The plasmasphere extends to about 4 R_E in the equatorial plane and since the plasmasphere is located close to Earth, where the exchange of momentum is large, the plasma co-rotates with the planet.

Surrounding the plasmasphere are the radiation belts located in two regions that extend from 2 to 6 R_E. The two distinct volumes show different properties where the inner radiation belt is populated with protons and the outer contains electrons with much lower energy content. The particles in the radiation belts are trapped in a periodic motion between two points of opposite latitudes on the two hemispheres. Due to the high energy content of the particles they constitute a hazard for spacecrafts and astronauts. In addition to the periodic motion between the two hemispheres the particles in the radiation belts precess around the globe. Due to the opposite charge, ions and electrons drift in different directions and leads to the creation of the *ring current* which is discussed below in Section 2.3.2.

2.2.2 The bow shock

The formation of collision-less bow shocks in front of magnetic obstacles had been theoretically predicted for a long time but the observation of a bow shock outside Earth's magnetosphere, made possible by in-situ measurements, was the

first proof that the phenomenon actually occurs. The solar wind is a collision-less plasma due to the very long mean-free path of the particles in it. Therefore, it was not clear if a collision-less bow shock could exist.

The bow shock is located a couple of R_E in front of the magnetopause and is only 100 - 1000 km thick. As the solar wind plasma travels across the bow shock the density and magnetic field increases while the velocity and Mach numbers decrease.

2.2.3 Pressure balance with the solar wind

The magnetosphere is not a static structure but varies slowly with the velocity and density of the solar wind and the strength of the geomagnetic field. The dynamic pressure from the solar wind is

$$p_{sw} = \rho_m v_{sw}^2 \tag{1}$$

where v_{sw} is the solar wind component normal to the magnetopause and ρ_m is the mass density. The pressure from an ideal dipole is

$$p_B = \frac{\mu_0 a^2}{32\pi^2 R^6} \tag{2}$$

where a is the magnetic moment of the dipole field of the Earth and R is the distance from the dipole. Equating the two pressures and solving for R results in an estimate of the distance to the magnetopause on the day side. Since electrons are so light the main contribution to the solar wind bulk pressure is made by protons and ions. Also, since the magnetic field of the solar wind is weak, the magnetic pressure of the solar wind can be neglected. At the flanks of the magnetopause, where the dynamic pressure is zero, it is the thermal pressure of the solar wind that balances the terrestrial magnetic pressure.

Inside the magnetosphere the relations are the opposite. Since the velocity decreases and the magnitude of the magnetic field increases the dynamic pressure can be neglected when compared to the magnetic pressure.

The distance to the magnetopause is about 10 R_E towards the Sun whereas the magnetosphere extends far beyond the lunar orbit on the night side. As discussed earlier, the distance to the magnetopause vary with several parameters and could in extreme cases reach the point where geosynchronous satellites are located. However, since the expression of the radius is a slowly changing function of density and velocity, any change of these variables must be large to significantly change the position of the magnetopause. The magnetosphere is a complex dynamic structure and a complete coverage of it lies outside the scope of this work.

2.2.4 ULF waves in the magnetosphere

Magnetic standing waves along the terrestrial magnetic field lines between the two hemispheres are called magnetic pulsations. This bouncing motion is made possible because the ionosphere act as a conducting surface. The reflectivity of the region in the ionosphere where the waves impinge, changes with the

evolution of the pulsation. Therefore, the waves can be detected by radar from Earth or by satellite by measuring this change of reflectivity.

These magnetic pulsations, or ULF waves, can either be continuous or irregular and are called Pc or Pi waves respectively. The waves are further categorized with respect to frequency. The general accepted ranges are shown in table 2.

	Pc-1	Pc-2	Pc-3	Pc-4	Pc-5
T(s)	0.2-5	5-10	10-45	45-150	150-600
f	0.2-5 Hz	0.1-0.2 Hz	22-100 mHz	7-22 mHz	2-7 mHz

Table 2: Ranges of Pc-5 pulsations (From Kivelson and Russel 1995)

A subset of the magnetic pulsations, some of which are further categorized as field lines resonances (or FLR), are believed to have their origin in the solar wind but the transmission of the source of these waves through the bow shock and the magnetopause is still little understood. One theory is that as the subsonic solar wind in the magnetosheath flows by the magnetopause it causes an instability (the Kelvin-Helmholtz instability) at the magnetopause surface. The instability results in the creation of compressional waves on the magnetopause surface which can be transmitted across the magnetic field lines to the point where the wavelength of the compressional wave matches that of the length of the field line. However, this theory should produce resonances at many frequencies and not in specific bands of frequencies which have been observed [25].

Another theory models part of the magnetosphere as a resonant cavity where waves with other frequencies than the resonant frequencies of the cavity is damped quickly. Resonant waves will then excite field line resonance in the same manner as in the first theory. This model could explain the bands of frequencies that have been observed.

Yet another notion is that MHD waves in the solar wind directly drives the pulsations. Only compressional waves are able to penetrate the bow shock and the magnetosheath so it is believed that the MHD waves in the solar wind are compressional [10].

As mentioned earlier Pc-5 waves in the magnetosphere seem to exist in some favorable bands of frequencies centered at 1.3, 1.9, 2.6 and 3.3 mHz but limited data sets (both in number and length) and also the type of technique used to measure the ULF-frequency, could mean that some results are related to large uncertainties [21][19]. In addition, the ULF waves are a result of MHD theory, a theory that does not include, for example, electron inertia. Therefore, arguments exists that show that the model itself is a bad representation of the environment related to the magnetosphere and that field line resonances does not exist in reality [2].

The magnetospheric ULF waves, in particular Pc-5 activity, can be of several different types but are generally said to be polodial, torodial or compressional corresponding to a disturbance in the magnetic field in the north-south, east-west and radial direction respectively. There also have been attempts to classify the polodial and torodial ULF waves regarding both their source and their location. Some results indicate that torodial ULF waves are more likely

to originate upstream (i.e. in the solar wind/magnetosheath or at the magnetopause/boundary layer which couples solar wind energy directly to the oscillation). The source for the polodial oscillations could be related to ring current injected ions [7][1].

2.3 Currents and particle flows in the magnetosphere

The different plasma populations in the magnetosphere are not static but dynamic in both space and time. The flow of charged particles always constitute an electric current which creates a magnetic field and thus makes the physics of the magnetosphere non-trivial since the created fields changes already existing fields. There are as many particle flows as there are plasma population in the magnetosphere and a complete coverage is outside the scope of this thesis and only the basic flows are illustrated in this section.

2.3.1 Magnetopause current

Although the solar wind flow behind the bow shock is subsonic and more turbulent than in front of the bow shock, the flow is still basically radially symmetric with respect to the Sun. The transition from the low magnetic field values in the solar wind (and behind the bow shock) to the large values found inside the magnetosphere requires a current flowing at the magnetopause surface. This current is related to the simple fact that ions (mostly protons) and electrons move in opposite direction when reaching the much larger magnetic field near the magnetopause. Thus, both particle types contribute to the electric current. This is illustrated in Figure 2.
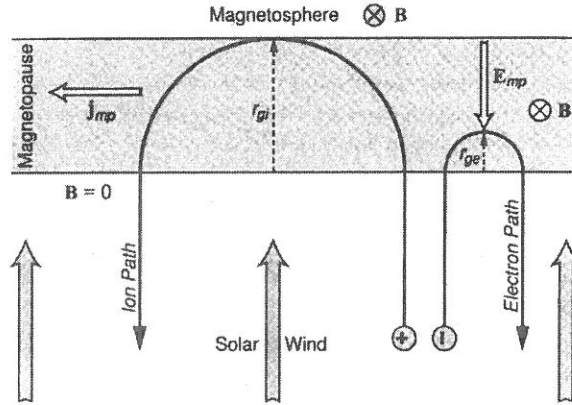

Figure 2: The reflection of electrons and ions at the magnetopause. r_{gi} is the gyro radius of ions (protons) and it can be seen that it's ions that determine the thickness of the magnetopause current layer.

It is clear that electrons have much smaller gyro radii (about 200 times smaller) because they are lighter than the ions and therefore the ions determine the thickness of the current layer. The effect of ions penetrating deeper

than electrons is that a polarization electric field is produced due to the charge separation. (Since the density of the solar wind is not constant, the charge separation varies with time and thus the electric field will also not be static. This produces a polarization gradient drift in the tangential direction as indicated by the electric field $\mathbf{E}_{mp}$ in Figure 2).

As shown in Figure 1 The magnetopause current flows from dawn to dusk. At higher (lower) latitudes the angle between the solar wind and the normal of the magnetopause increases and the terrestrial magnetic field also changes appearance from being perpendicular to the solar wind stream to having components parallel (anti-parallel) with it. On the day-side of the Earth the magnetopause current is split into a northern and southern lobe. On both the lobes the current flow in the same direction. The resulting magnetic field created by the current *contribute* to the total terrestrial magnetic field.

2.3.2   Ring current

As mentioned in Section 2.2.1 the radiation belts consist mostly of ions and electrons. In addition to their bouncing motion the particles also have a drift component. Since ions and electrons drift in different directions the radiation belts also carry a westward directed current called the *ring current*. The ring current produces a magnetic field which is opposite of and *counteracts* the terrestrial magnetic field Earthward of the ring current. The particle drift velocity in the ring current is a rapidly decreasing function with increasing latitude, as is their number density. Therefore, most of the ring current is concentrated at low latitudes.

2.3.3   Neutral sheet current

Dividing the two magnetospheric lobes on the night side is the neutral sheet carrying a current directed from dawn to dusk. This current is related to the plasma pressure gradient, directed southward in the northern lobe and northward in the southern, i.e., toward the neutral sheet. Compared to the different plasma population in the magnetotail, the density and temperature of the neutral sheet plasma is therefore quite high.

2.3.4   Magnetosheath flow

Behind the bow shock, in the magnetosheath, the solar wind has slowed down to subsonic values and is denser and hotter than outside the bow shock. The magnetic field in this region is also larger and more irregular. The particle stream flow around the magnetopause and creates a stagnation point on the Earth-Sun line where the flow is split between the two hemispheres. The subsonic stream is, due to the nozzle effect (see [5] for example), again accelerated to supersonic velocity at the sides of the magnetopause [30]. The magnetosheath flow is of interest partly due to the Kelvin-Helmholtz instability (cf. Section 2.2.4) as the source for some of the observed magnetospheric ULF waves.

2.4 Magnetic pulsations in the solar wind

On large scales the solar wind can be modelled as a conducting fluid where the governing factors essentially are Newton's laws of motion and Maxwell's equations. The mechanical and electromagnetic forces interact with each other and the result is a wave phenomena called magnetohydrodynamic (MHD) waves. The basic MHD equations are:

$$\rho_m \frac{d\mathbf{v}}{dt} = \mathbf{i} \times \mathbf{B} - \nabla p \tag{3}$$

$$\mathbf{i} = \sigma(\mathbf{E} + \mathbf{v} \times \mathbf{B}) \tag{4}$$

$$-\frac{\delta \varrho}{\delta t} = \nabla \cdot \varrho \mathbf{v} \tag{5}$$

$$\nabla \times \mathbf{B} = \mu_0 \mathbf{i} + \frac{1}{c^2} \frac{\delta \mathbf{E}}{\delta t} \tag{6}$$

$$\nabla \times \mathbf{E} = -\frac{\delta \mathbf{B}}{\delta t} \tag{7}$$

$$\nabla \cdot \mathbf{B} = 0 \tag{8}$$

$$p = const \cdot \rho_m^\gamma \tag{9}$$

where ρ_m is the mass density, $\mathbf{v}$ is the velocity, $\mathbf{i}$ is the current density, $\mathbf{B}$ is the magnetic flux density, p is the pressure, σ is the conductivity, $\mathbf{E}$ the electric field, ϱ is the charge density and γ is a constant.

Using linear approximation, meaning that a disturbance, if it exists, is small compared to that of the ambient (static) variables, and discarding higher order terms, the above equations can be combined to form a homogenous set of linear equations. The result can be written

$$\begin{bmatrix} \omega^2 - v_A^2 k_{||}^2 - c_{ms}^2 k_\perp^2 & 0 & -c_s^2 k_{||} k_\perp \\ 0 & \omega^2 - v_A^2 k_{||}^2 & 0 \\ -c_s^2 k_{||} k_\perp & 0 & \omega^2 - c_s^2 k_{||}^2 \end{bmatrix} \begin{bmatrix} \delta v_{0x} \\ \delta v_{0y} \\ \delta v_{0||} \end{bmatrix} = 0$$

where $v_A = B/\sqrt{\mu_o \rho_m}$, $c_{ms} = \sqrt{c_s^2 + v_A^2}$, δv_{oi} is the amplitude of the resulting wave in the x, y and parallel direction respectively. c_s is the speed of sound and is defined as $c_s = \sqrt{\gamma p/\rho_m}$ where p is the pressure of the plasma, ρ is the mass density and γ is the polytropic index. The assumed geometry is that the background magnetic field is directed as $\mathbf{B_0} = B_0 \hat{\mathbf{e}}_{||}$. The wave vector is $\mathbf{k} = k_{||} \hat{\mathbf{e}}_{||} + k_\perp \hat{\mathbf{e}}_x$.

2.4.1 Shear Alfvénic waves

For the disturbance in the y-direction the dispersion relation is

$$\omega_A = \pm k_{\parallel} v_A \tag{10}$$

and describes a wave travelling parallel or anti-parallel to the ambient field and creating a disturbance perpendicular both to the wave vector and to the ambient magnetic field. Because the disturbance is transverse the Alfvén wave does not, to the first order, change the total magnetic field. This can be shown by considering the total magnetic field

$$|\mathbf{B}|^2 = |\mathbf{B_0} + \delta\mathbf{b}|^2 = \mathrm{B_0}^2 + (\delta\mathrm{b})^2 \approx \mathrm{B_0}^2 \tag{11}$$

2.4.2 Magnetoacoustic waves

Having looked at the disturbance in the perpendicular direction focus here is on the remaining two directions. If the direction of propagation is perpendicular to the ambient magnetic field (i.e. $k = k_{\perp}$) the dispersion relation is

$$\omega^2 = k^2(c_s^2 + v_A^2) \tag{12}$$

which represent a *fast* wave travelling perpendicular to the ambient magnetic field (i.e. $k = k_{\parallel}$) with phase velocity $V = \sqrt{(c_s^2 + v_A^2)}$

If the propagation is parallel to the ambient magnetic field then the dispersion relation is

$$\omega^2 = \frac{1}{2}k^2(c_s^2 + v_A^2 \pm (c_s^2 - v_A^2)) \tag{13}$$

which represent a *slow* wave. When $v_A > c_s$ the slow wave represent a sound wave with phase velocity c_s and the fast wave has phase velocity v_A. For the opposite case the fast wave has phase velocity c_s and the slow wave has phase velocity v_A. At all times, the Alfvén waves has phase velocities intermediate of the slow and fast wave. The fast and slow waves are also called compressional (magnetoacoustic) waves since they change the magnetic pressure.

2.4.3 On modal power in the interplanetary magnetic field

The question whether the interplanetary magnetic field actually contains modal power have been discussed for many years and additional controversy has been added when some reports indicate that solar g- and p-modes are a source for pulsations in the solar wind. It has been suggested that the interplanetary magnetic field indeed has a large amount of modal power and that the picture of the solar wind as a purely stochastic medium have to be abandoned [28][29][27][15]. The source of the waves is in general believed to be related to the Sun and its surroundings in some way. Interestingly, the solar pressure modes frequencies match those in the Pc-5 frequency range [12]. However, the discussion continues as problems exist regarding the data analysis technique being used [18]. Especially the ability of different types of power spectra, basically a mathematical construction which is based on the assumption of repeating sinusoidal functions, have been discussed. All in all, a consensus whether or not the solar

15

wind magnetic field, or any related variable, contains modal power is established. However, the source of the pulsations and the nature of the different wave phenomena still need investigation.

Besides the obvious 11 year solar cycle and the 27 day rotational cycle of the Sun there also have been numerous reports of solar wind variations with periodicities of, for example, 16, 10.6, 9.6, 5.5, 1.7, 1.3, 0.5 and 0.3 years, 180, 154 , 73, 51 and 14 days. Also, periodicities corresponding to solar g- and p-modes have been reported. Interesting for the 1.3 year pulsation is that there also seem to exist a 1.3 year time variation in the cosmic ray periodicity. Also, evidence of a period of 1.3 year seems to exist in the convection zone of the Sun. Only the north-south component of the magnetic field in the solar wind seem to be affected by this 1.3 year periodicity [4].

2.4.4   Turbulence or quasi-periodic activity?

For the random appearance of the magnetic field in the solar wind, a distinction between turbulence and an actual wave must be made. Even if some spectra appear to have a narrow-bandwidth signal, in many cases this can not be seen in the corresponding time series. Therefore, such events should not necessarily be interpreted as pulsations. Basically, several periods of a wave should be seen to make the assumption of wave activity. The variability of the solar wind parameters and their connection to either turbulence or "waves" have for example been discussed by Goldstein [6] and Mullan [13]. In this work, turbulence is defined as wave activity with very short duration. Turbulence would not show a distinct peak but rather show a flat spectra or a spectra of many peaks of similar magnitudes.

Of course, one could discuss the connection between turbulence and actual waves. In many cases turbulence could be the source of wave activity. For example, an event of a shorter period of turbulence which resembles wave activity could in interaction with the magnetosphere, act as a short initial pulse with a longer representation of wave activity in the magnetosphere. Then the observation is considered a wave but the source is not. In many cases, like the Kelvin-Helmholtz instability at the magnetopause, turbulence *and/or* wave activity could be the source of the instability, indicating that turbulence not at all is less important than wave activity for the understanding of magnetospheric physics in the solar wind.

16

3 Instrumentation and data availability

The ACE satellite orbits the L1 Lagrangian point located on the Earth-Sun line about 1.5 million km from Earth (roughly 1 % of the distance to the Sun). It is well outside the magnetosphere and makes correlation between solar wind parameters and parameters inside the magnetosphere possible.

The magnetic field experiment (MAG) on ACE consists of two triaxial flux-gate magnetometers located on booms extending 4.19 m on each side of the spacecraft. Such sensors are also used for the Magnetic Field Investigation (MFI) on the WIND satellite. This type of sensors has proved cheap, reliable, low-power consuming and very accurate. They have previously been used (and are used) for the Voyager, ISPM, GIOTTO, Mars Observer and Mars Surveyer missions. The instrumentation characteristics are summarized in table 3 [24].

Range:	0.001 - 65536 nT
Bandwidth:	12 Hz
Noise level:	0.006 nT RMS in 0-10 Hz
Sampling rate:	3, 4 or 6 samples/s

Table 3: Summary of MAG instrument characteristics

3.1 Data availability

The two sensors on ACE provide very accurate and reliable measurements of the magnetic field. Rarely does the instrument fail and often the corrupt data consists of only one data point which is easy to approximate with linear interpolation. When segments of data points are missing no interpolation can be done and the data set must be discarded. However, depending on the study being done, interpolation over longer periods of missing data points could be an appropriate method. When observing quasi-periodic waves in the solar wind this can not be done since this method could introduce spurious frequencies in spectra.

The missing data points could of course be due to real physical events where the instrument is saturated or unable to switch range mode fast enough. The second and third cause for missing data points could be due to system failure in ACE instrument control or transmission failure. Saturation of the magnetometers are unlikely since the range is extremely wide. Therefore, the shorter segments of missing data points are likely to be of artificial origin and not due to real physical events in the solar wind. In this study, longer segments of missing data points results in the period being completely discarded.

Table 4 displays the number of missing data points for each year for the MAG instrument on ACE. For the early part of the mission, especially for 1998, the number of missing data points were large. Since the discarded time is proportional to the number of missing data points one would expect that the number of events related to pulsations in this year are somewhat lower than for other years with more complete data coverage.

17

Year	N_{bad}/N_{total}
1997	0.08
1998	0.01
1999	< 0.001
2000	<0.001
2001	<0.001
2002	<0.001
2003	0.001
2004	<0.001

Table 4: Percentage of bad data points for MAG instrument

For 1997 and 2004 the number of bad data points have been multiplied with $365/N_{days}$, where N_{days} is the available number of days in the data set. This is done because the data sets for 1997 and 2004 do not include the entire year in this study.

3.2 ACE position and limited data sets

In 1997 ACE was en route to the L1 Lagrangian point and therefore measurements during this period can not be considered reliable data for comparisons with other measurements made later in the mission. Care should then be taken when comparing results from 1997 with results from other years. From late 1997 and from then on, ACE was in orbit around the L1 Lagrangian point. The orbit basically lies in the ecliptic plane but deviate somewhat in latitude.

4 Method of analysis

The mathematical construction of power spectra is a powerful tool to represent the frequency content of a signal. The estimation or calculation of power spectra are a complicated matter and are the subject of entire books and therefore a complete coverage lies outside the scope of this thesis. Because of its complicated nature, care must be taken when using power spectra as it is easy to make the assumption that if a power spectra shows a clear peak it then must be relevant. This is often not the case and spectra must often be compared to the time series it represents. In an early stage in this work test trials were carried out to observe what kind of different power spectra was produced with different constructed time series. Of special interest are time series which show large and rapid changes since a quickly changing signal represent high frequency components in the frequency domain. Rapid and large changes of many variables including the magnetic field can often be seen in the solar wind. Therefore, a study of this kind is interesting to conduct since the foundation of this thesis is based on the "validity" of power spectra. The results of the study can be found in Appendix A.

4.1 Calculation of power spectra

Several features in the magnetic field of the solar wind leads to a distortion of the spectra and to overcome the possibility of identifying frequency components which are in some way artificial, an average method is often used where the spectra of several overlapping time series are averaged together. This lowers the number of data points used and thus also the resolution of the spectra but can effectively eliminate artificial frequencies introduced by the spectral analysis. Also, an averaging method lowers the error in estimation by $1/\sqrt{N}$ where N is the number of averages. However, in this study, the main analysis is made on a non-averaging method where spectra for 6 hours are calculated.

Two approaches can be used when calculating power spectra: parametric and nonparametric methods. The parametric methods make assumptions regarding the time series observed and then in a least-mean-square sense minimizes the error to this assumed model [17]. For the solar wind this is probably not a good method since the solar wind variables show a very random behaviour. A general model is therefore difficult to assign to, for example, the magnetic field or density variations in the solar wind. For a very long data set, on the order of days to years, the solar wind magnetic field have been found to satisfies the condition of "weak" stationarity [6]. For a shorter time series this is simply not the case. Therefore, parametric methods should not result in more "valid" power spectra than non-parametric methods for the short time series in this study.

One way to determine that a spectral peak is 'real' and, in some way, linked to a longer duration of wave activity, several spectra with different resolution can be calculated. In addition to the spectra calculated over 6 hours, five 2 hour spectra are calculated during the 6 hour period. When the frequencies of one or more of the 2 hour spectra matches those of the 6 hour spectrum the probability of wave activity should be higher for this time period. The reliability of this method to accurately distinguish events of interest is unknown. However, it is in some sense a better estimate compared to that of only using a single time

period. It is also more likely that the wave activity in the solar wind show a shorter duration than 6 hour. Events of shorter duration will never the less also be visible in a 6 hour spectrum so it is assumed that this is an appropriate length of choice.

In this study, spectra that have one or two clearly distinguishable spectral peaks are chosen for further analysis. Therefore, the events in this study should represent periods where a simple relationship exists between the variables in the solar wind. If the largest and second largest peak in a spectra has peak magnitudes P_i and P_{i+1} respectively, the spectra are considered interesting if $P_i/P_{i+1} > \delta$ holds. The setting of δ is varied. For a study of two clear peaks then the third peak must also be considered.

This method were used on two frequency spans in the Pc-5 vicinity. The lower frequency span (LFS) was located at 1-10 mHz and the upper frequency span (UFS) was located at 1.7-17.0 mHz.

4.2 The use of tapers

When extracting a short time series out of a larger data set one will have to deal with the problem of the start and end of the time series not having the same value. Since the mathematical representation of a time series to the Fourier transform consist of many time series in a row, the mismatch between the start and end of the primary data set will introduce high frequency components and distort the produced spectra. To overcome this problem one could simply add a "flipped" data set to the end of the primary data set. In most cases however, tapers are multiplied to the signal prior to transformation. Several different tapers, also called *windows* , can be used depending on the desired character of the produced spectra. For most purposes, and in this work, a Hanning window is considered sufficient since it is generally believed to be a good all-purpose window. More advanced methods, like multi-taper techniques, have also been used when studying solar wind parameters. The method involves several tapers of different properties which are multiplied to different parts of the signal prior to transformation.

The difficulty in choosing an appropriate spectral analysis method to determine periodic features in the solar wind is noted.

Multiplying a time series with a taper forces the start and end of the series towards zero. This means that if a signal exists near the start or end of the series this signal will be greatly reduced in amplitude and maybe not show up at all in spectra. To overcome this problem an overlap of data sets must be done. In this study a 50 % overlap is made dividing each day into seven 6 hour periods and two 3 hour periods. The spectra are however always computed for 6 hour time periods. By zero-padding the signal prior to the multiplication with the Hanning window, more information is made available for the spectral analysis. This is due to that a disturbance close to the start or end still keeps some energy and are not force to zero using this method. This was also done for the periods in this study. The zero-padded length was 1 hour and the length of the Hanning window was equal to the zero-padded time series.

4.3 Frequency resolution and bandwidth of the MAG-instrument

For the ACE MAG data used the magnetic field has a time resolution of 16 s. The measured value is actually a mean value of many more samples being taken a number of times every second depending on the current range mode of the instrument (cf. Table 3). The Nyquist frequency is 31.5 mHz and for a study of waves in the Pc-5 vicinity the bandwidth is clearly sufficient.

The frequency resolution Δf is related to the length of the time period as $\Delta f = 1/(2T)$ where T is the length of the time period. For a 6 hour period $\Delta f \approx 0.02$ mHz. Making T three times shorter results in a 3 times worse resolution of 0.08 mHz which is the case for a 2 hour spectral analysis. For a study in the Pc-5 domain a resolution lower than 0.1 mHz introduces, with respect to the frequency span, quite a large uncertainty.

4.4 Summary of method of analysis

To summarize, power spectra of magnetic field data sets of 6 hours with 16 s resolution were calculated for the duration from 1997 to 2004. The analysis used a 50 % overlap of periods and no filters were applied to the time series prior to transformation. The magnetic field $B(t)$ was zero-padded where the length of the padding was 1 hr. The mean of the 6 hour period was then removed from the zero-padded magnetic field $B(t)$. It was then multiplied with a Hanning window $W(t)$ of the same length and the power spectra of the resulting product were calculated.

The resulting power spectra were then examined for one or two dominant peaks in two frequency spans and is summarized in Table 4.4 below.

Frequency span (mHz)	Designation
1-10	LFS (Lower frequency span)
1.7-17.0	UFS (Upper frequency span)

Table 5: The definition of the two frequency spans used in the study and their designations.

In each calculated power spectra those with one or two dominant peaks are chosen for further analyses. This means that the events in this study are representative for the very simplest wave phenomena where a clear observation of wave activity at one or two frequencies is possible. If the first and second most dominant peaks have peak amplitudes P_i and P_{i+1} respectively, then periods where $P_i/P_{i+1} > \delta$ holds, are selected. The value of δ is also varied and is defined as 3, 2.5, 2 for the one-peak study and 1.7, 1.6, 1.5 for the two-peak study.

The selection of δ is of course arbitrary and has been made so as to produce a reasonable amount of selected data sets. For the 6 hour analysis with a 50 % overlap between periods, each year amount to a total number of approximately 2840 periods. The triggered events should be much lower than this value to rule out the effect of randomness.

Defining the width of a peak is difficult and should basically be related to the properties of the type of spectra being calculated. Since the resolution is 0.02 mHz this is the narrowest peak width possible. However, peaks of various widths exist in calculated spectra and a definition of a region around each peak must be made which is discriminated in the comparison. Therefore, a peak is defined as having the largest peak amplitude and that the surrounding data points also relate to the actual peak. This makes sense as it is difficult to separate periodicities with frequencies very close to each other. In this study the peak width is defined as being approximately 0.1 mHz.

In addition to the method described above, at least for the one-peak study, an additional criterion can be matched to select the spectrum as interesting. If a clear peak is visible but $P_i/P_{i+1} < \delta$, the spectra is still selected if the modal power in this clear peak is considered as large compared to the mean power in the current frequency span. This additional criterion triggers several events were the first analysis failed.

5 Results

For the events with a spectrum that matches the criteria with one or two peaks that are clearly larger than the spectra in general, the total number of events during each year of the mission is calculated. Because 1997 and 2004 contains (in this this study the data set for 2004 extended up to September) fewer days in the data set, the total number of events for these two years was scaled with the factor $365/N_{days}$ where N_{days} is the available number of days in the data set.

The relative difference δ between the peak amplitude of the largest peak and the second largest peak in the calculated power spectra was chosen, for both frequency spans, to identify a reasonable total number of events during one year. The largest difference, corresponding to the highest value of δ, should result in enough events that could prove fruitful for a statistical analysis. The lowest difference in peak amplitude should result in many more events, but not so many so that a random choice of periods would yield a similar result. The third and intermediate difference setting was chosen as the average of the largest and lowest setting. For the analysis for two clear peaks in spectra, using the method described results in values of δ that lie very close to each other. Since the different settings of δ lies so close a clear distinction between these events are difficult to make, at least with respect to the amplitude of the pulsations. Figure 3 and Figure 4 below show the distribution of events during the mission for the three settings of δ. 1997 and 2004 were scaled in the same manner as described in Section 3.1

The solar cycle was at its maximum at year 2000/2001 and in the beginning of the ACE mission the solar cycle had just passed its minimum value. One might expect a larger number of events occurring at solar maxima based on the assumption that solar wind pulsations, as depicted in this study, are more likely to occur during times when the sunspot number is large. However, it is difficult to see the 11 year solar cycle in either of Figure 3 or Figure 4
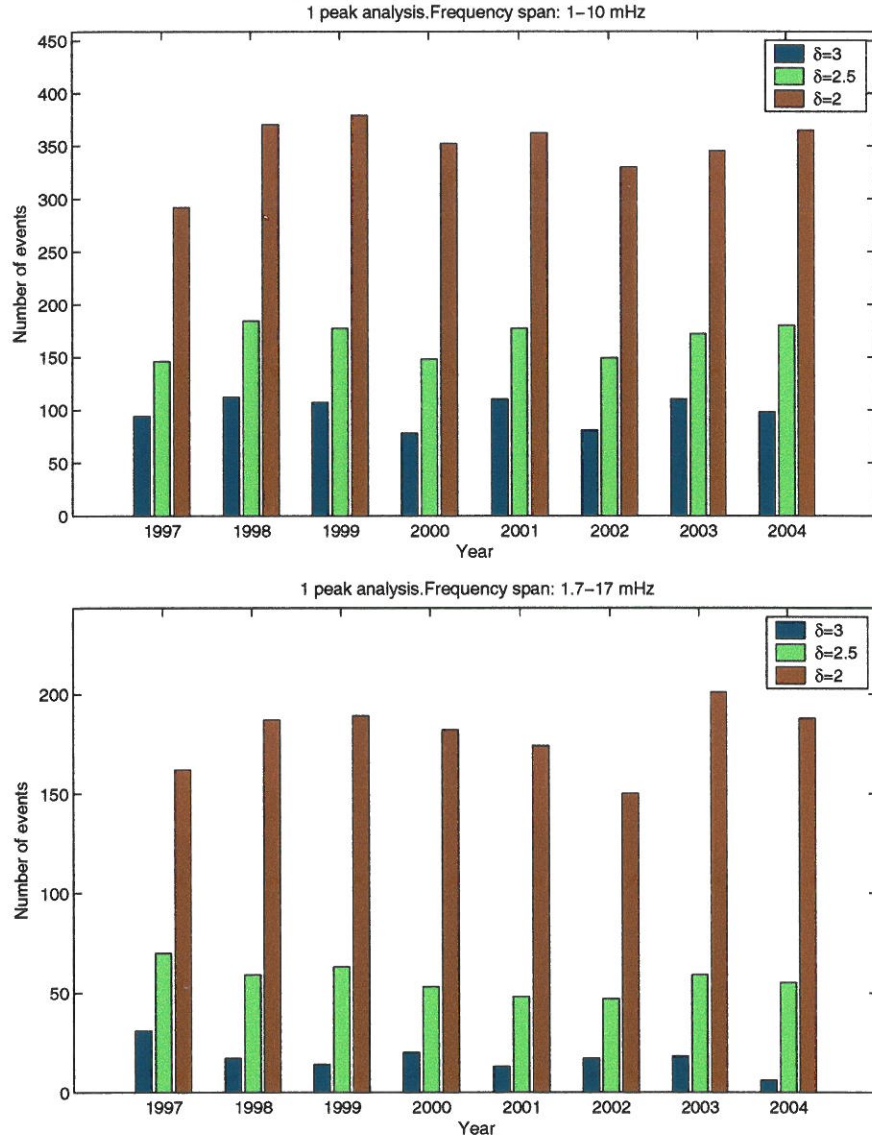
Figure 3: The top diagram shows the number of events for the one-peak analysis and for the lower frequency range and the lower diagram shows the corresponding distribution for the higher frequency span.
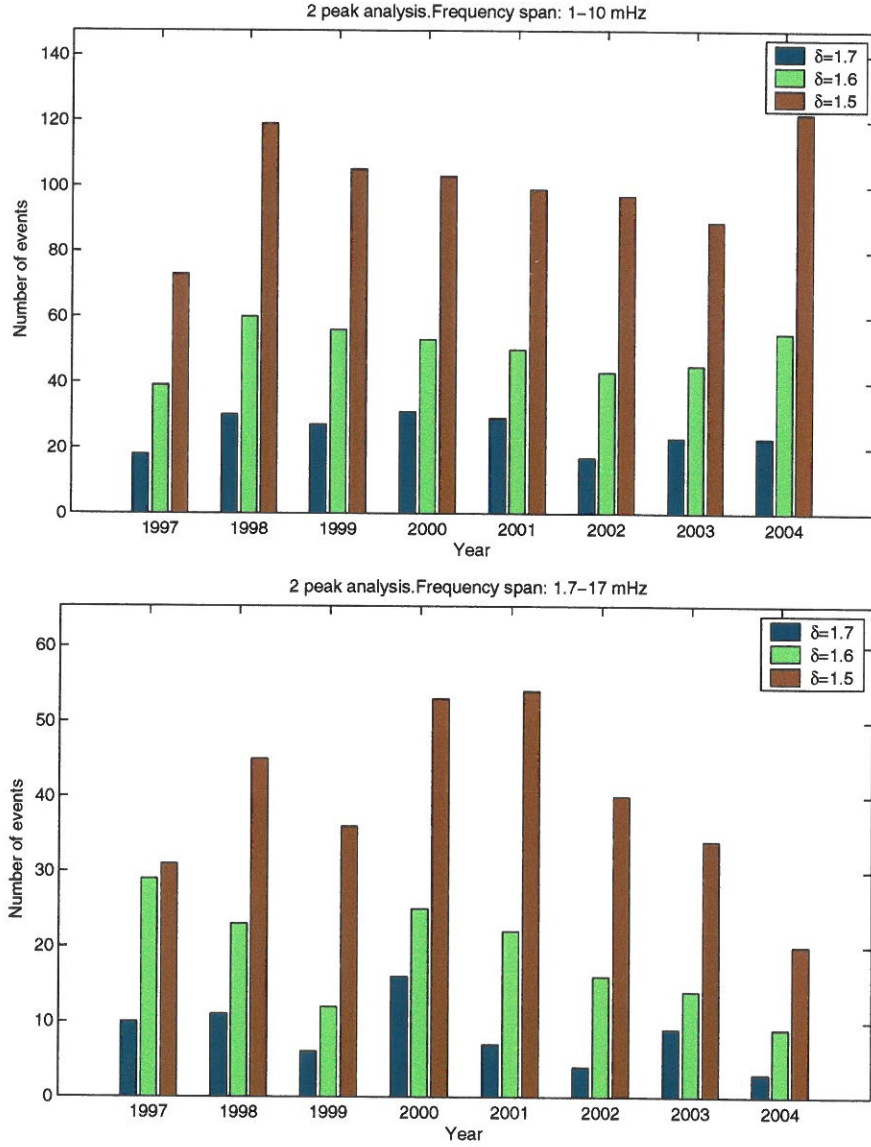
Figure 4: The corresponding analysis for the two-peak criterion. The top diagram shows the occurrence for the lower frequency span and the lower diagram shows the corresponding distribution for the higher frequency span.

The bottom diagram in Figure 4 and the upper diagram in Figure 3 are the only distribution diagrams that show any relation to the 11 year solar cycle. However, it is not clear how this type of analysis actually fit to the assumption that there actually is an increase of *clear* or *simple* wave activity during solar maxima. The method is unable to distinguish turbulent events where many strong periodicities occur at the same time. So it is possible that the produced spectra in this study is solar cycle independent since it is unable to clearly show the clear 11 year solar dependence with respect of occurrence.

It is also possible that a spectral analysis of the data set would prove more fruitful to observe the 11 year variation of the Sun. Figure 3 and 4 indicate that the modal power in the solar wind, at least for the events studied in this work, do not vary with the solar cycle. The occurrence of clear wave phenomena do not change on these large time-scales but are related to shorter periods.

5.1 Indications of a 29 day variation related to solar wind streams

No or little evidence was found in this study regarding the periodicity of the 11 year cycle of the Sun. Another study regarding the 27 day periodicity related to the rotation of the Sun was also made.

Wave activity related to the boundaries and the interior of high speed solar wind streams should show this variation because the life span of coronal holes associated with high speed solar wind streams often have a life span longer than 27 days. Therefore, for a time series of almost eight years, a monthly periodicity should be possible to observe under the assumptions made. However, new coronal holes are also constantly created and the complete picture is quite complicated.

The occurrence distribution of the events over the entire data span from 1997 to 2004 were calculated. A 150 hour running box-car average were applied to the data and the resulting occurrence diagram and its normalized spectrum can be seen in Figure 5. When calculating the spectra the mean of the entire time span was removed and a Hanning window was applied to the data set prior to transformation.
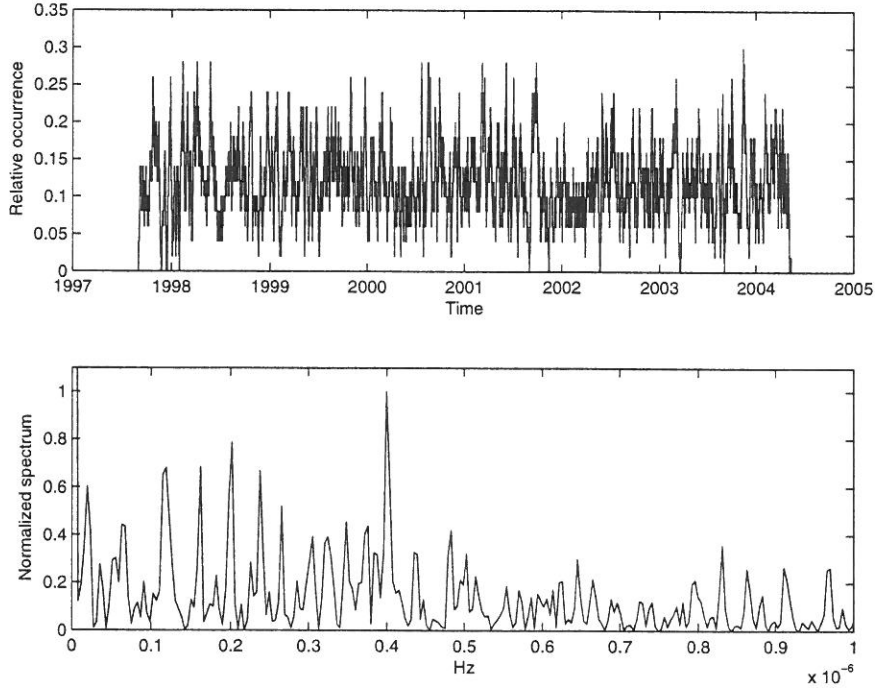
Figure 5: The top diagram shows the (relative) occurrence for the events in this study for 1997-2004. The lower diagram is the normalized spectrum of the same period. This study was made for the lower frequency span of 1-10 mHz and for one peak. A 0.4 μHz peak can clearly be seen.

In the spectrum in Figure 5 a clear peak is visible near 0.4 μHz corresponding to a 29 day periodicity. Several smaller peaks can also be seen around 0.12,

0.15, 0.2 and 0.24 μHz corresponding to a variation of 96, 77, 58 and 48 days respectively. However, their relevance have not been confirmed so they could be artificial peaks or peaks related with large uncertainties. Also, occurrence rate distributions were calculated for each year. Although not all years shows a good correlation with the 0.4 μHz peak, many do as in the example below for 2000 and 2001 shown in Figure 6
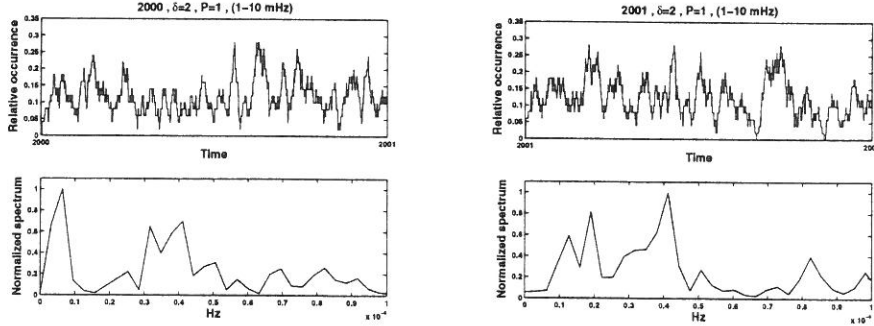

Figure 6: The left diagram shows the occurrence rate for 2000 and the right for 2001. The lower panel is the normalized spectrum of the corresponding period in the panel above. Again, the 0.4 μHz peak can clearly be seen although the resolution in a one-year study is much worse than for the time series in Figure 5.

The same analysis was also done for the higher frequency span of 1.7-17.0 mHz which showed similar results although the peak at 0.4 μHz for the longer data set was not as clear as in Figure 5. For the analysis made on each year the result was similar to the analysis made for LFS. A clear peak at 0.4 μHz for at least 3 of the eight years were found. For year 2000 spectra for both UFS and LFS indicate a 0.4 μHz peak and spectra for LFS indicate a peak for 2001 but UFS does not. 2003 also showed a clear peak for UFS. It is interesting to notice that these clear peaks were more visible during the solar maxima at around 2000 and 2001 than for other years (except for 2003). The spectra for years 2000 and 2003 is shown as examples in Figure 7.

The right diagram in Figure 7 also show small peaks at 0.12 and 0.23 μHz. The peak at 0.20 μHz were also clearly visible for the years 1998 (0.23 μHz), 1999 (0.25 μHz for LFS and 0.23 μHz for UFS) and 2001 (0.20 μHz). The peak at around 0.12 μHz was also visible in five of the yearly spectra calculated for 1998 (0.10 μHz), 2000 (0.12 μHz) and 2001 (0.12 μHz for LFS and 0.10 μHz for UFS). As for the example for the 0.4 μHz peak the 0.12 μHz peak were more pronounced during solar maxima.

The results indicate that many of these persistent spectral peaks, observed in spectra are more likely to happen during solar maxima. However, the uncertainty related to this investigation is large and the frequency resolution would be preferred to be higher to make a definite conclusion.
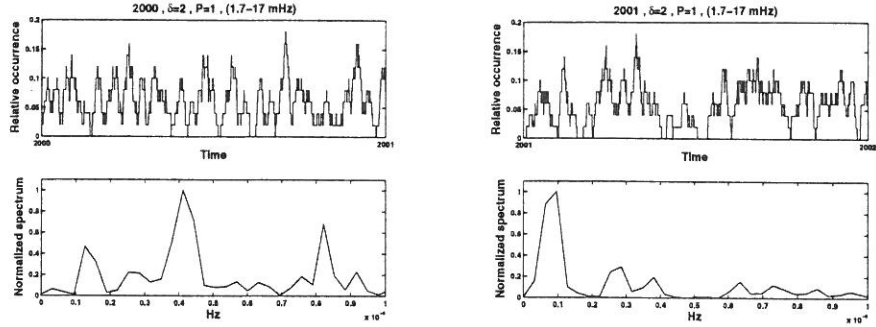
Figure 7: The left diagram is for 2000 and the right for 2003. Clear peaks in the vicinity of 0.4 μHz can be seen.

5.2 Indications of a 1.4 year solar variability

Similar to the analysis made when examining the 27 day rotational cycle of the Sun another study was made regarding the 1.3/1.4 year periodicity. This variation has been reported by others and have been mentioned earlier in Section 2.4.3. The data analysis was basically the same as for the analysis for the 27 day cycle in Section 5.1. Here an average method was used when calculating the spectrum. The length of the averaged spectra was 2/3 of the entire period of approximately 8 years.

The running mean used were approximately 100 days long to remove the effects of the 27 day solar rotational cycle. The mean of the period was then removed and a Hanning window was applied prior to transformation of all of the spectra used in the averaging process. The resulting occurrence diagram and its spectrum are shown in Figure 5.2
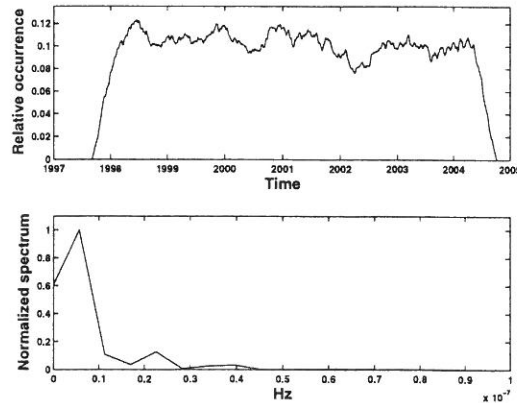
Figure 8: The top diagram shows the occurrence over the entire lifespan of ACE. The lower diagram is the normalized average spectrum of the same period. This study was made for the lower frequency span of 1-10 mHz and for one peak. δ was set to its lowest value of 2.

29

The large peak around 5.6 nHz is probable to be of artificial origin. The spectrum shown is an average of several spectra where each spectrum corresponds to a time series which is 2/3 of the entire time span in length. This time series corresponds to approximately a 5.3 year variation which is in the vicinity of the large peak seen.

An additional peak is seen at 23 nHz corresponding to a 1.4 year variation. Although difficult to see in Figure 5.2 the peak is persistent with varying lengths of the running box-car average and also using different non-averaging spectral methods. Therefore, it is believed, at least for this frequency span and settings of δ, that the peak indicate a variation of approximately 1.4 years related to some physical mechanism on the Sun. However, the resolution in this particular study is low.

In Figure 5.2 the analysis was made for the lower frequency span. For the higher frequency span a small peak was found at 17 nHz. The resolution for the average spectrum was approximately 5.6 nHz so the peak corresponds to a change by only one data point of that of the location of the 23 nHz peak. Therefore, the peak seen are related to a very large uncertainty. For a study of a nearly yearly variation a longer time span than 8 years would be preferred.

5.3 Frequency distribution

Frequency distribution diagrams were calculated for the events in each year. The frequency is that of the main peak (and the secondary peak for the two-peak analysis) and the bin-width was set to 0.1 mHz. Frequency distribution diagrams was also constructed for all the events during the entire ACE mission and is shown in Figure 9 below. The Figure shows only the complete frequency distribution for δ=2. Several more frequency distributions diagrams can be found in Appendix B.
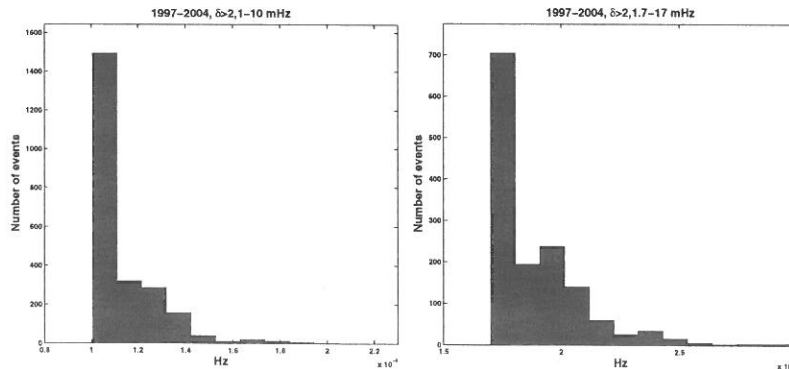

Figure 9: Frequency distributions diagrams for LFS (left) and UFS (right), δ=2 and for the one-peak analysis.

The large bin for the lowest frequency in the range is expected since a "normal" 6 hour spectra would have be exponentially decreasing for increasing frequencies. All the frequency distribution diagrams, where δ has the value of 2.5 or 3, have the same slope as the diagrams in Figure 9. In any frequency span, the lowest

frequency has the largest probability of being selected as the highest peak in the span.

Comparing the two frequency spans the number of events is lower for UFS than for LFS. This have also been previously noted regarding the number of events for each year in Section 5. No special differences can be seen when comparing the frequency distributions for different settings on δ indicating that there is no discrepancy in frequency between disturbances with peaks of relative large modal power and peaks with smaller relative modal power.

The frequency distribution diagrams for the two-peak analysis were similar to that of the one-peak study. No particular frequency is predominant during the events in this study and the appearance of the diagrams are similar as for the one-peak study.

5.4 Directional properties of the magnetic field

The angles of the mean total magnetic field during the events were calculated and polar histograms of the resulting angles in the XY-plane (the ecliptic plane) and the YZ-plane (in GSE-coordinates) were constructed. The analysis was made for every year and for all settings of δ for both frequency spans. Only the angles for the one-peak analysis for the entire mission is shown here in Figure 10. The yearly mean angles of the total magnetic field can be found in Appendix C.
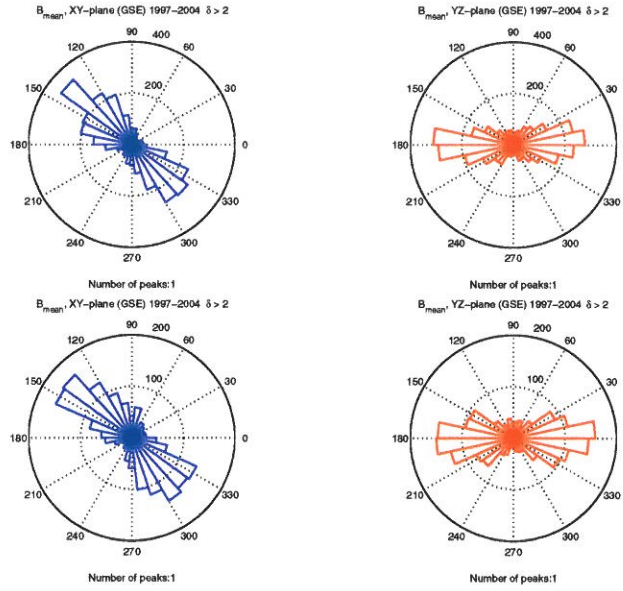
Figure 10: The top diagram shows the angular distribution of the total magnetic field in the XY-plane (blue) and the YZ-plane (red) for the lower frequency span of 1-10 mHz. The bottom diagram is the corresponding analysis for the higher frequency span of 1.7-17.0 mHz. 0 degrees in the YZ-diagram corresponds to a northward directed total magnetic field. The XY-diagram should be imagined as the ecliptic plane where the Sun is to the left and the Earth at the right.

The distribution during the events show similar results for all years and comparisons between the lower frequency span and the higher frequency span also seem to indicate no differences. Except perhaps for the events during 1998 where both frequency spans indicate events where the magnetic z-component of the magnetic field were mostly south-ward. The angle in the XY-plane were also more perpendicular (towards 270 degrees) and somewhat more radial (towards 150 degrees) instead of the expected angle of 135 or -45 degrees. Perhaps many of the events for this year were concentrated at times where solar wind features were similar. Since B_z were mostly south-ward for these events they are especially interesting for correlation with Pc-5 field-line-resonances in the magnetosphere. The different appearance for 1998 is also indicated in the two-peak analysis. The polar plots for 1998 can be found in Appendix C in Figures

27 and 29. Figure 10 shows that the mean angle of the total magnetic field during the events in this study is not different from that of the mean calculated over a long time. Therefore, the events in this study are not biased toward any particular angle of the total magnetic field. They instead show the property of occurring with equal probability for all angles of the total magnetic field.

5.5   Main direction of the disturbances

Any of the three components in the magnetic field **B** could be related to the disturbance seen in the magnitude of the magnetic field B. In addition, a wave phenomena changing several of the magnetic field components would mean that it is the sum of two or all of the components that contribute to the peak.

To investigate which one of the components of the magnetic field that were responsible for the peak seen in the spectrum for B the same analysis were conducted for the components of the magnetic field as was done for the magnitude of the magnetic field. The analysis was made for the one-peak study where $\delta = 2$.

The frequency of the maximum peak found for either of the three magnetic field components were compared to the frequency f_B of the maximum peak found for B. The setting P_i/P_{i+1} was set to a lower value of 1.5 since the location of the largest peak is somewhat more important here than the peak ratio. The results can be seen in table 6.

	LFS (1-10 mHz)	UFS (1.7-17 mHz)
N	1911	1143
B_x (%)	3.9	3.1
B_y (%)	3.8	1.6
B_z (%)	4.2	2.6
B_x and B_y (%)	0.1	0.1
B_x and B_z (%)	0.2	0.1
B_y and B_z (%)	0.2	0

Table 6: The first row shows the total number N of triggered events during 1997-2004 for the two frequency spans, the next three rows indicate the percentage of the events that showed a peak at f_B for the specific component. The three rows at the bottom lists events that had two components that showed a peak at f_B

The absolute majority of the events show no spectral peak (or it's not the peak of greatest magnitude in the spectra) at f_B. The main contribution to the peak seen in B must therefore be made by the sum of two or all of the magnetic field components. No component contributes more than the others and events where two components show a peak at f_B are very few indeed.

It is noted that this analysis is made in absolute coordinates (GSE) and a study of the disturbance parallel and perpendicular to the mean magnetic field during the period could be more appealing. Also, the length of the period could also be a factor that severely alters these results. A 6 hour period could be considered a too long time span for the disturbances observed. In addition, the spectral peaks of the components must be located at exactly (within 1 %) of f_B

to be considered as a main magnetic component responsible for the disturbance in this study. A peak outside this range could have energy "leaking" into the area around f_B. Therefore, the uncertainty related to the percentage figures in Table 6 is quite high.

6   Conclusions and discussion

Although the statistical basis to observe the 11 year solar cycle in this study is quite small, the variation can still be seen in at least two of the occurrence diagrams in Figure 3 and Figure 4. In Figure 3 the variation can be seen for the analysis made for one peak for the lower frequency span and in Figure 4 the variation is observed for the two-peak analysis for the higher frequency span. No discrepancy can therefore be found between the two frequency spans related to the 11 year solar cycle. This indicate that wave phenomena, as depicted in this study, are as likely to happen in either of the two frequency spans.

The number of events in Figure 3 for the lower frequency span (LFS) indicate a larger number of events than for the higher frequency span (UFS). Large amplitude waves are often associated with large spectral peaks and they tend also to exist at low frequencies. Therefore, for the low frequency span the probability of a smaller disturbance to be the dominant peak is lower than for the higher frequency span.

The frequency distributions of the events in this study show that no particular frequency is predominant. The large number of pulsations with frequency close to the lower cutoff frequency is expected, due to the mean appearance of a typical power spectrum for the periods observed in this study. Further, no discrepancy in frequency can be found between the events in the two frequency spans examined. The distributions are similar with a tendency for the events in the higher frequency span to be spread out over a wider frequency range. Since the number of events for LFS are higher than for UFS this can not be considered to be a result of different statistical basis. It is believed that this also can be connected to the typical appearance of a power spectra of the kinds used in the study.

A 29 day variation, possible connected to the rotational cycle of the Sun and to solar wind streams, is observed in this study as discussed in Section 5.1. The observations show an increase of clear wave activity with a 29 day periodicity which corresponds to a frequency of 0.4 μHz which is indicated in, for instance, Figure 5. The variation can be observed since a positive correlation exists between the free energy density and compressional areas in the solar wind. These areas have been disturbed from their local equilibrium and the probability of an increase of wave phenomena is therefore higher in these regions than in rarefaction areas. The availability of free energy is bound to create many different wave phenomena and also turbulence. Some of the waves exist for time periods where one wave phenomena show one or two particular frequencies that are more dominant than others. And it is these events that are found in this study. Highly turbulent regions would often show spectra where many frequencies exist at the same time and is therefore not triggered as an event with the method used. However, it is likely that these regions in the solar wind also are more turbulent than rarefaction areas. Pulsations with very short duration is also considered a "wave" in this work and therefore the duration of the waves in this study range from fractions of an hour to several hours.

The rotational cycle of the Sun varies with latitude and since the measurements were made on the Sun-Earth line this should correspond to the variation for low solar latitudes. The result is consistent with earlier results. Several other small peaks are also found in the analysis but their relevance are difficult to determine. The peak at 0.12 μHz have been reported by others and corresponds to a period of 0.3 years. For instance El-Borie et al. showed that a small 0.3 year variation was found to exist in the solar wind ion density [4].

The spectral peak seen at 23 nHz in Figure 5.2 indicate a variation of 1.4 year related to some solar mechanism. Several other observations of the same variation have been made. Paularena et al. have for example related a 1.3 year variation in the north-south component of the magnetic field to the same periodicity in the ap-index [16]. In this study only perturbations related to changes of the magnitude of the magnetic field field were considered, so for this study the variation in B_z is still unknown since either component of the magnetic field could be responsible for the perturbations.

A spectral analysis of each of the components of these time scales would be interesting to conduct and might prove to be an interesting follow-up to this work.

The mean angles of the total magnetic field during the events are similar to that of the mean angles calculated over a very long period in the solar wind. However, for 1998 the angular distribution was spread out over a wider range of angles. This could be related to a few similar events occurring during this year. A more detailed analysis of the solar wind parameters during these events would be an interesting task. Since B_z was mostly south-ward during 1998 these events are somewhat more interesting than others regarding the coupling between the solar wind and the magnetosphere. The conclusion has to be that pulsations, as depicted in this study, in the magnetic field magnitude are as likely to happen for any mean angle of the magnetic field. The events are not biased toward any particular angle but instead show the property of occurring with equal probability for all angles of the total magnetic field.

The modal power contained in the peaks found in the magnetic field magnitude B was caused by a disturbance in all of the magnetic components. For the events where only one component contributed more than the others no specific component contributed more. About 1-5 % of the events had a spectral peak which was exactly at the location of the frequency f_B of the main peak seen in B. A very small percentage (< 0.3 %) of the events showed spectral peaks at f_B where two components contributed to the peak (i.e. they had the same main peak frequency). However, a study of the disturbances perpendicular and parallel to the total magnetic field would be more interesting as it has been shown that many of the disturbances in the solar wind are transverse to the total magnetic field.

References

[1] B. J. Anderson. An Overview of Spacecraft Observations of 10 s to 600 s Period Magnetic Pulsations in the Earth's Magnetosphere. In *Solar Wind Sources of Magnetospheric Ultra-Low-Frequency Waves*, pages 25-+, 1994.

[2] P. M. Bellan. Mode conversion into non-MHD waves at the Alfvén layer: The case against the field line resonance concept. *Journal of Geophysical Research (Space Physics)*, 101:24887–24898, November 1996.

[3] Richard C. Carrington. Description of a singular appearance seen in the Sun on September 1. *Mon. Not. R. Astron. Soc., (reprinted by Meadows, A. J., Early Solar Physics, p. 181, Pergamon, New York, 1970)*, 20:13–15, 1860.

[4] M. A. El-Borie. On Long-Term Periodicities In The Solar-Wind Ion Density and Speed Measurements During The Period 1973-2000. *Solar Physics*, 208:345–358, August 2002.

[5] C. G. Fälthammar. *Space Physics*. 1994.

[6] M. L. Goldstein, D. A. Roberts, and W. H. Matthaeus. Magnetohydrodynamic Turbulence In The Solar Wind. *Annual Review of Astronomy and Astrophysics*, 33:283–326, 1995.

[7] Denton R. Lessard M. Miftakhova E. Hudson, M. and R. Anderson. A study of Pc-5 ULF oscillations. *Annales Geophysicae*, 22:289–302, January 2004.

[8] V. Izmodenov, G. Gloeckler, and Y. Malama. When will Voyager 1 and 2 cross the termination shock? *Geophysical Research Letters*, 30:3–1, April 2003.

[9] Adolph S. Jursa, editor. *Handbook of Geophysics and the space environment*. 1985.

[10] L. Kepko, H. E. Spence, and H. J. Singer. ULF waves in the solar wind as direct drivers of magnetospheric pulsations. *Geophysical Research Letters*, 29:39–1, April 2002.

[11] Decker R. B. Hill M. E. Armstrong T. P. Gloeckler G. Hamilton D. C. Lanzerotti L. J. Krimigis, S. M. and E. C. Roelof. Voyager 1 exited the solar wind at a distance of ˜85AU from the Sun. *Nature*, 426:45–48, November 2003.

[12] K. G. Libbrecht, M. F. Woodard, and J. M. Kaufman. Frequencies of solar oscillations. *Astrophysical Journal Supplement Series*, 74:1129–1149, December 1990.

[13] Smith C. W. Ness N. F. Mullan, D. J. and R. M. Skoug. Short-Period Magnetic Fluctuations in Advanced Composition Explorer Solar Wind Data: Evidence for Anticorrelation with Alfvén Speed. *Astrophysical Journal*, 583:496–505, January 2003.

[14] Brittnacher M. Chua D. Fillingim M. Parks, G., G. Germany, and J. Spann. Behavior of the aurora during 10-12 May, 1999 when the solar wind nearly disappeared. *Geophysical Research Letters*, 27:4033–4036, December 2000.

[15] K. I. Paularena. An investigation into solar wind plasma periodicities. *Journal of Geophysical Research (Space Physics)*, 101:27533–27542, December 1996.

[16] Szabo A. Paularena, K. I. and J. D. Richardson. Coincident 1.3-year periodicities in the ap geomagnetic index and the solar wind. *Geophysical Research Letters*, 22:3001–3004, 1995.

[17] D. B. "Percival and A. T." Walden. *Spectral analysis for physical applications, Multitaper and conventional univariate techniques*. 1993.

[18] P. Riley and C. P. Sonett. Interplanetary observations of solar g-mode oscillations? *Geophysical Research Letters*, 23:1541–1544, 1996.

[19] J. M. Ruohoniemi, R. A. Greenwald, K. B. Baker, and J. C. Samson. HF radar observations of Pc 5 field line resonances in the midnight/early morning MLT sector. *Journal of Geophysical Research (Space Physics)*, 96:15697–+, September 1991.

[20] Edward Sabine. On periodical laws discoverable in the mean effects of the larger magnetic disturbances. *Philos. Trans. R. Soc. London*, 142:103–124, 1852.

[21] J. C. Samson, R. A. Greenwald, J. M. Ruohoniemi, T. J. Hughes, and D. D. Wallis. Magnetometer and radar observations of magnetohydrodynamic cavity modes in the Earth's magnetosphere. *Canadian Journal of Physics*, 69:929–937, September 1991.

[22] Gosling J. T. Steinberg J. T. McComas D. J. Smith C. W. Ness N. F. Hu Q. Skoug, R. M. and L. F. Burlaga. Extremely high speed solar wind: 29-30 October 2003. *Journal of Geophysical Research (Space Physics)*, 109:9102–+, September 2004.

[23] Steinberg J. T. Gosling J. T. McComas D. J. Smith C. W. Ness N. F. Hu Q. Skoug, R. M. and L. F. Burlaga. Extremely fast solar wind observations during October-November, 2003. *AGU Spring Meeting Abstracts*, pages A3+, May 2004.

[24] L'Heureux J. Ness N. F. Acua M. H. Burlaga L. F. Scheifele J. Smith, C. W. The ace magnetic fields experiment. *Space Science Reviews*, 86:613, 1998.

[25] D. J. Southwood. Some features of field line resonances in the magnetosphere. *Planetary and Space Science*, 22:483–491, March 1974.

[26] D. P. Stern. A brief history of magnetospheric physics before the spaceflight era. *Reviews of Geophysics*, 27:103, 1989.

[27] D. J. Thomson, L. J. Lanzerotti, and C. G. Maclennan. Interplanetary magnetic field: Statistical properties and discrete modes. *Journal of Geophysical Research (Space Physics)*, 106:15941–15962, August 2001.

[28] D. J. Thomson, L. J. Lanzerotti, and C. G. Maclennan. Studies of some statistics of the interplanetary magnetic field and implications for discrete modes. *Advances in Space Research*, 29:1911–1916, 2002.

[29] D. J. Thomson, C. G. Maclennan, and L. J. Lanzerotti. Propagation of Solar Oscillations Through the Interplanetary Medium. *Nature*, 376:139–+, July 1995.

[30] A. D. M. Walker. Excitation of field line resonances by MHD waves originating in the solar wind. *Journal of Geophysical Research (Space Physics)*, pages 38–1, December 2002.

A. Certain features in the solar wind magnetic field and spectral analysis

There are many different features in the solar wind which can cause problem in spectral analysis. Several of these problems have been listed earlier in this thesis. 4.1 A limited study have been made that investigate what impact certain features in the magnetic field of the solar wind can have on the power spectra of. These features include

- A peak structure

- A step structure

- Variations of the two above

The third feature could for example be a longer period with a distinct elevated magnetic field or an inverted peak or step structure of varying lengths and magnitudes. Three typical structures are shown below.
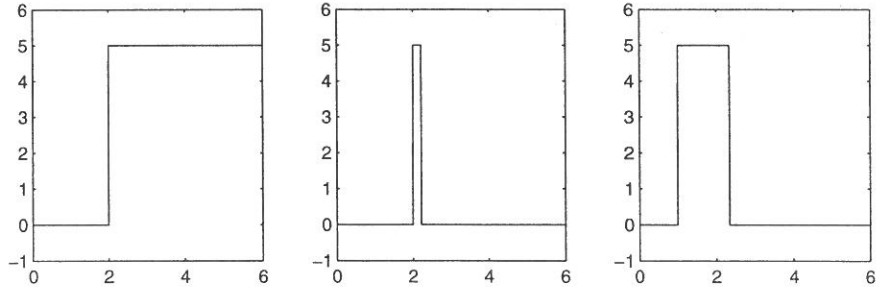
Figure 11: Three typical features of the magnetic field in the solar wind. A *step*, a *peak* and a longer peak.

It is more than likely that a multitude of sinusoidal signals could exists at the same time in the solar wind affecting many of the parameters and also, for example, the magnetic field. Constructing an artificial signal as

$$\sum_{i=1}^{N} a_i sin(\omega_i t) + D + n \tag{14}$$

where N is the number of simultaneous signals with angular frequencies ω_i and amplitudes a_i and D is some clear feature, or disturbance of some kind, and n is random normal distributed noise. D is one of the three features described in Figure 11 above. All of them are examples of time series that could distort power spectra and lead to misinterpretation of spectral peaks. The use of filters could also introduce spurious peaks in the resulting power spectra as is discussed below.

The artificial signal is constructed of 5 sinusoidal functions with the frequencies and amplitudes shown in table 7.

i	a_i	f_i (mHz)	ϕ (rad)
1	1	0.3	0
2	0.8	0.7	$\pi/3$
3	0.6	1.6	$-\pi/4$
4	0.4	2.3	$3\pi/2$
5	0.2	3.4	π

Table 7: Characteristics of the long artificial signal

The above signal is persistent throughout the entire 6 hour period and therefor a shorter signal was also added and the characteristics of the shorter signal is listed in table 8.

i	a_i	f_i (mHz)	ϕ (rad)
1	2	0.5	$-2\pi/3$
2	1	1.3	$\pi/4$
3	0.5	2.7	$-\pi/2$

Table 8: Characteristics of the short artificial signal. This shorter signal is 2 hours in length.

The short signal is located at the same place in the time series to indicate a heightened level of wave activity. The length of the short signal are two hours. The noise variable n are pseudo-random normal distributed numbers with a maximum value of 1. Clearly, this is a noisy signal.

Below are some example of solar wind features that complicate spectral analysis.
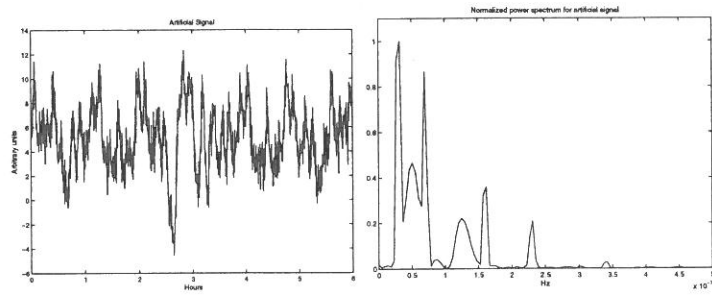
Figure 12: To the left is the constructed signal and its normalized power density spectra to the right.
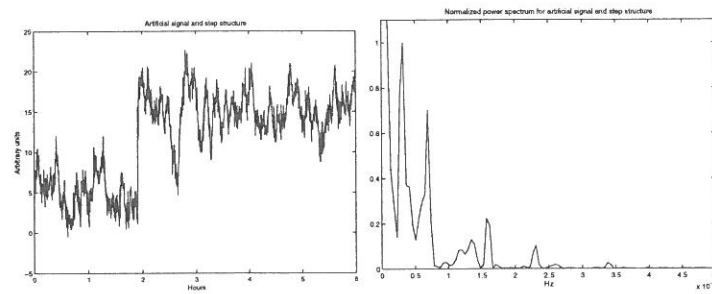
Figure 13: Signal with a step appearance and its spectrum. The noise spectral density is the same as for Figure 12
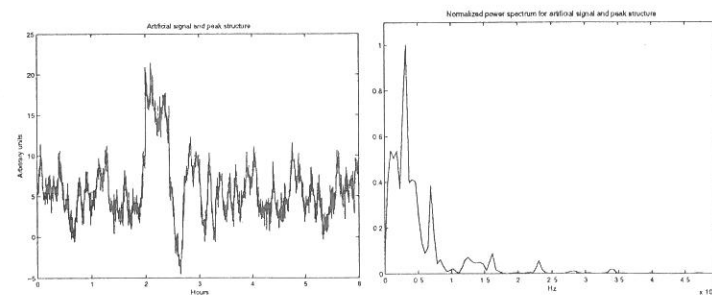
Figure 14: Signal with a distinct peak and its spectrum.
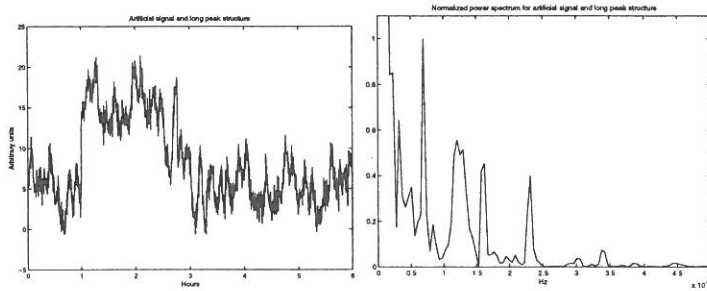
Figure 15: Signal with a long distinct peak and its spectrum.

For the undisturbed signal in Figure 12 all peaks are visible in the spectrum except the short low amplitude signal at 3.4 mHz. It is obvious that a SNR-value of 1 is too low for a short-lived periodicity to be distinguishable in a 6 hour spectra. A longer signal, such as the signal at 3.4 mHz, extending over the whole period and at this signal-to-noise ratio, contains enough energy to be seen in the spectrum.

In Figure 13 the spectrum now holds a considerable amount of energy for low frequencies corresponding to a DC-level. Removing the 6 hour mean of such a time series could make normalizing difficult. Further more, the short signal at 0.5 mHz would be difficult to detect in this spectra since it seems to have merged with the peak at 0.3 mHz. In addition, the clear peak from Figure 12 at 1.3 mHz has here split into two frequencies. In Figure 14 the situation is basically the same although the DC-level has dropped considerable as expected.

In Figure 15 where the peak is a bit longer and more resembling a step structure the spectra is radically different. A strong DC-level is expected but the importance of the short signal at 1.3 mHz is overstated, probably due to one *unfortunate* realization of the ensemble of normal distributed noise. In addition a spurious frequency is located at 0.9 mHz clearly indicating that the peak at 3.4 mHz has no meaning. At least at this SNR.

Running box-car averages and power spectra

A running box-car average, of some certain length, is often used to remove the dc-level of a signal. Since this basically is a low-pass filtering process it results in a high-pass filtering upon subtraction. In addition, Thomson et al. [28] state that results can be totally misinterpreted when using running box-car averages and that the results may not at all represent an underlying physical process. Further, making a running mean of a very dynamic time series, such as the three structures listed above, and trying to remove the trend of the period is a difficult task and could result in distorted spectra. Therefore, care must be taken when using this method. A large DC-level can be accepted as long as the spectra are properly normalized. For a very quiet period, a running box-car average could result in a clearer view of underlying wave activity compared to that a simple mean value of the whole period. But since the problems involved with this type of averaging together with spectral analysis are severe, a more simplified approach has been taken. In this study only the total 6 hour mean

42

value has been subtracted from each data point in the period as mentioned in Section 4.4.

Wave or turbulence?

The duration of the wave activities in the solar wind are unclear. There have been reports of pulsations with a manifold of frequencies. There is also the problem with separating wave activity from turbulence as mentioned in 2.4.4. For an activity to be labelled *a pseudo-sinusoidal wave* in the solar wind the number of periods should at least be more than four. However, wave activity in the magnetic field in the solar wind are often very hard to see without first using a narrow band-pass filter. Therefore, this study of true sinusoidal signals extending during the entire 6 hour time period are likely to be a bad representation of wave activity in the solar wind. The study made in this appendix should instead be considered as a test of the hypothesis for the ability of a simple power spectral technique to clearly show spectral content for a time series that is 6 hour long.

Spectral analysis and filters

A filtering process of a time series could very well introduce spurious frequencies of artificial origin due to the limitations of the constructed filter. In an initial study a bandpass filter was applied to known time series of data imitating a typical solar wind magnetic field time series. Much like the time series shown in this appendix in Figure 13, 14 and 15. It was seen that in many cases where the data set showed rapid and large changes, the filter introduced artificial peaks in spectra. Of course, if the real pulsation is strong, and occur over a longer period, the peaks introduced by the filter is of little importance due to the very large difference in peak amplitude. However, for low amplitude pulsations, occurring over shorter periods of time, the filter induced spectral peaks could easily be mistaken for a real peak. In an automated technique, where large data amounts are processed, it is impossible to go through the time series manually and properly identifying real peaks. However, a shorter interval could be examined manually and it could then be assumed that the statistics for the entire period is similar. In this work, no filter is applied before the calculation of power spectra.

Even without filters, rapid and large changes in solar wind variables could, by mistake, be interpreted as real peaks. This is duly noted as well. One can discuss if periods that show rapid and large alteration should be discarded but then a very large number of periods with potential pulsations in it would be neglected. Pulsations often occur when magnetic data show these appearances since energy is available to any physical process that can restore equilibrium. In this study, no periods are discarded due to rapid and large variations in solar wind variables. Only longer periods of bad data points are the cause for discarding data sets where interpolation is questionable.

B. Frequency distribution

Lower Frequency span (1.0-10.0 mHz) - one-peak analysis

In the figure below frequency distribution diagrams for 1997-2004 for LFS for all the different settings on δ are shown. The widths of the bins are 0.1 mHz. No wave phenomena with a certain frequency seem to occur more often than others, at least at this bin-width. The size of the bin furthest to the left is explained by the appearance of a typical 6 hour magnetic field spectrum.

The yearly frequency distributions for this one-peak analysis can be found in the following pages in this Appendix.
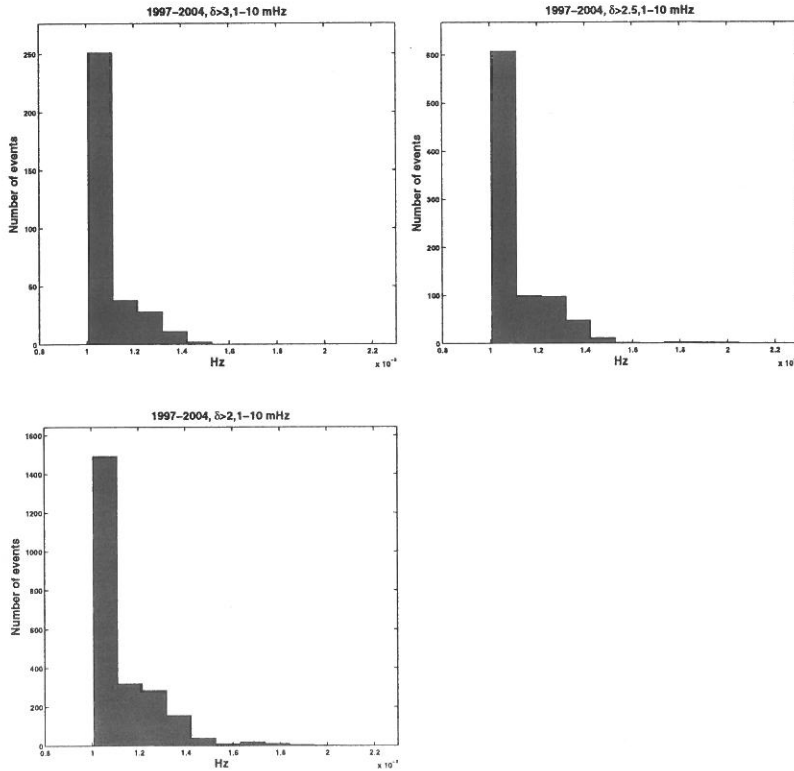
Figure 16: Frequency distribution for the events during 1997-2004 for the lower frequency span (LFS) and for the one-peak analysis.
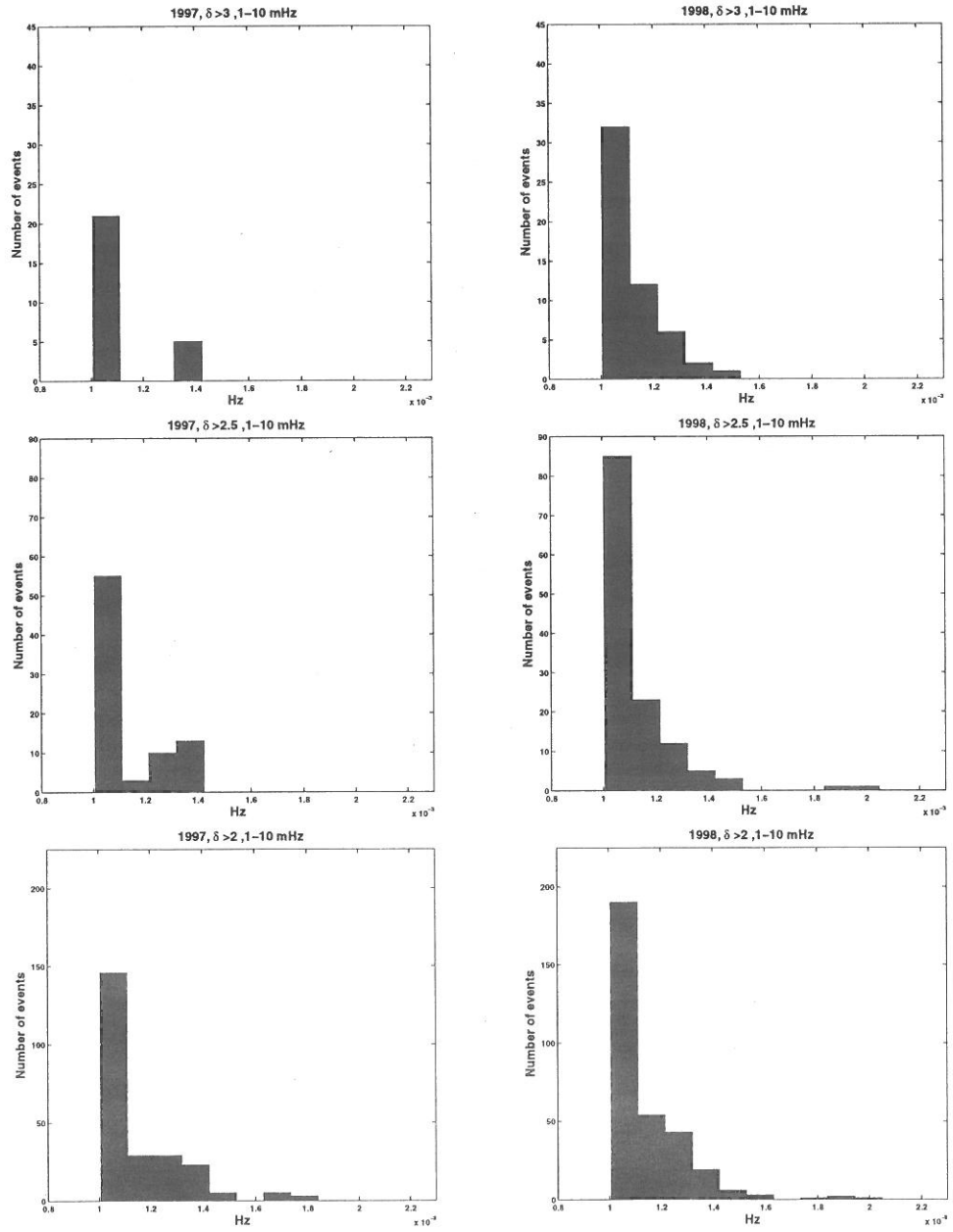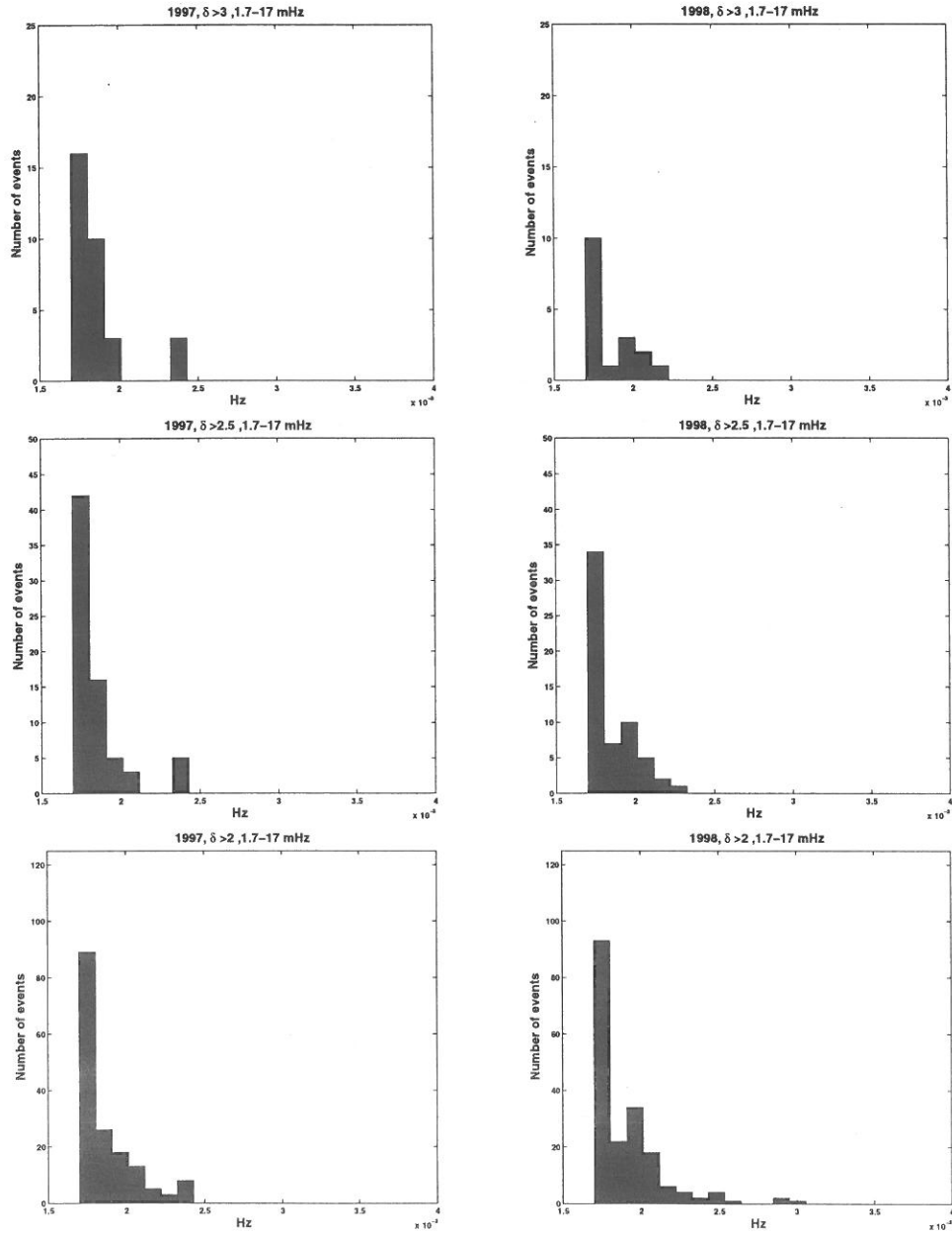
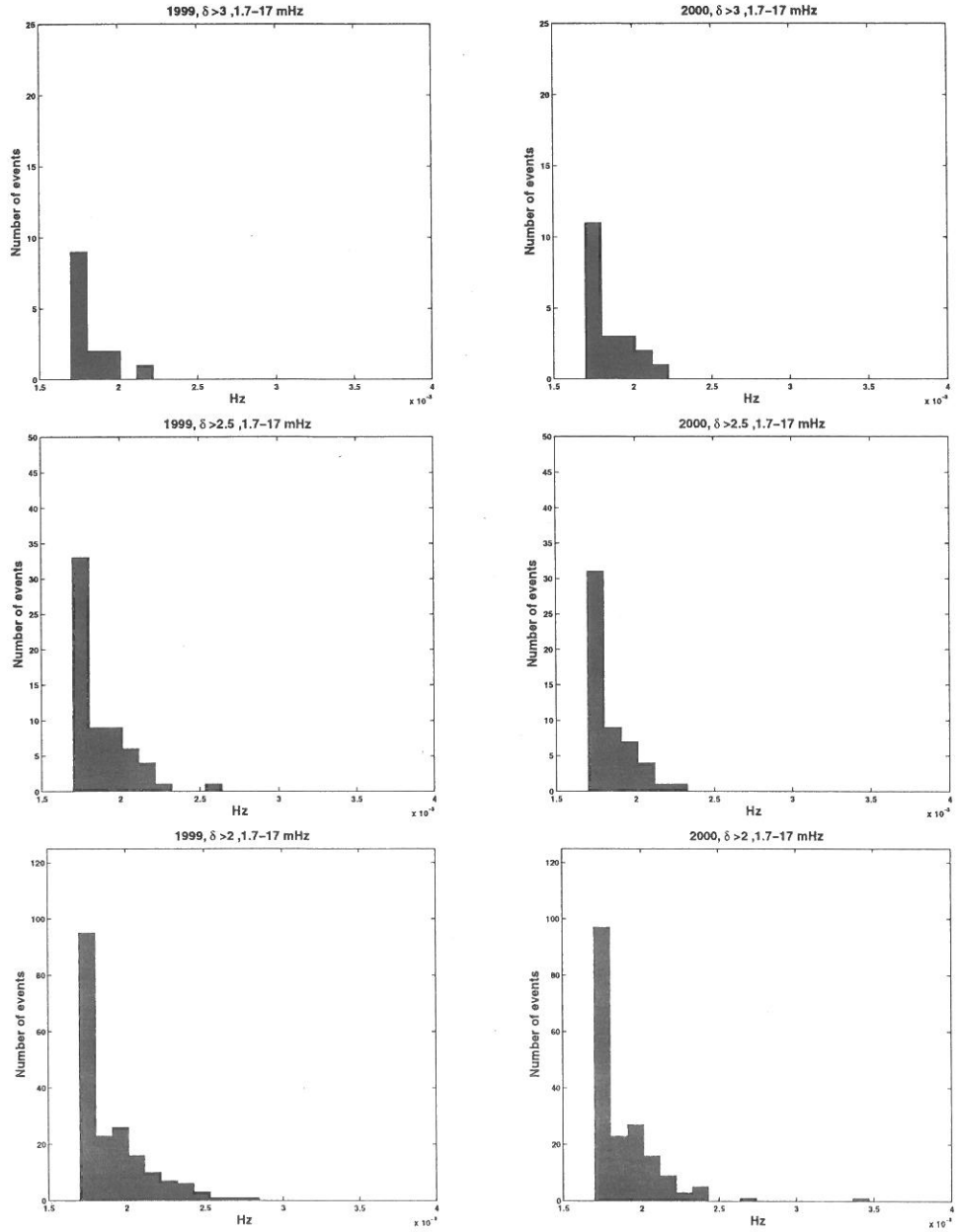Figure 17: Frequency distribution of the events during 1997 and 1998.
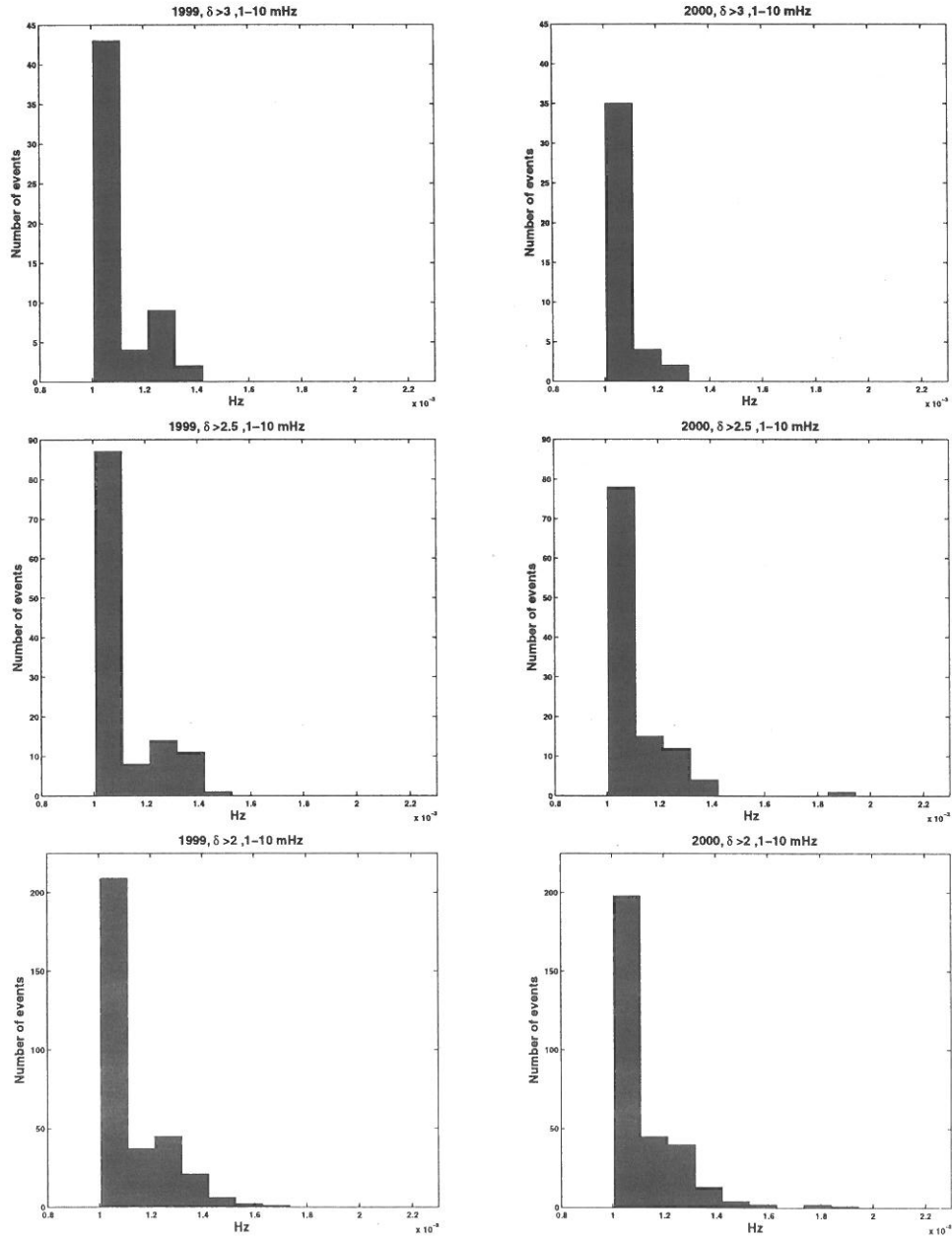
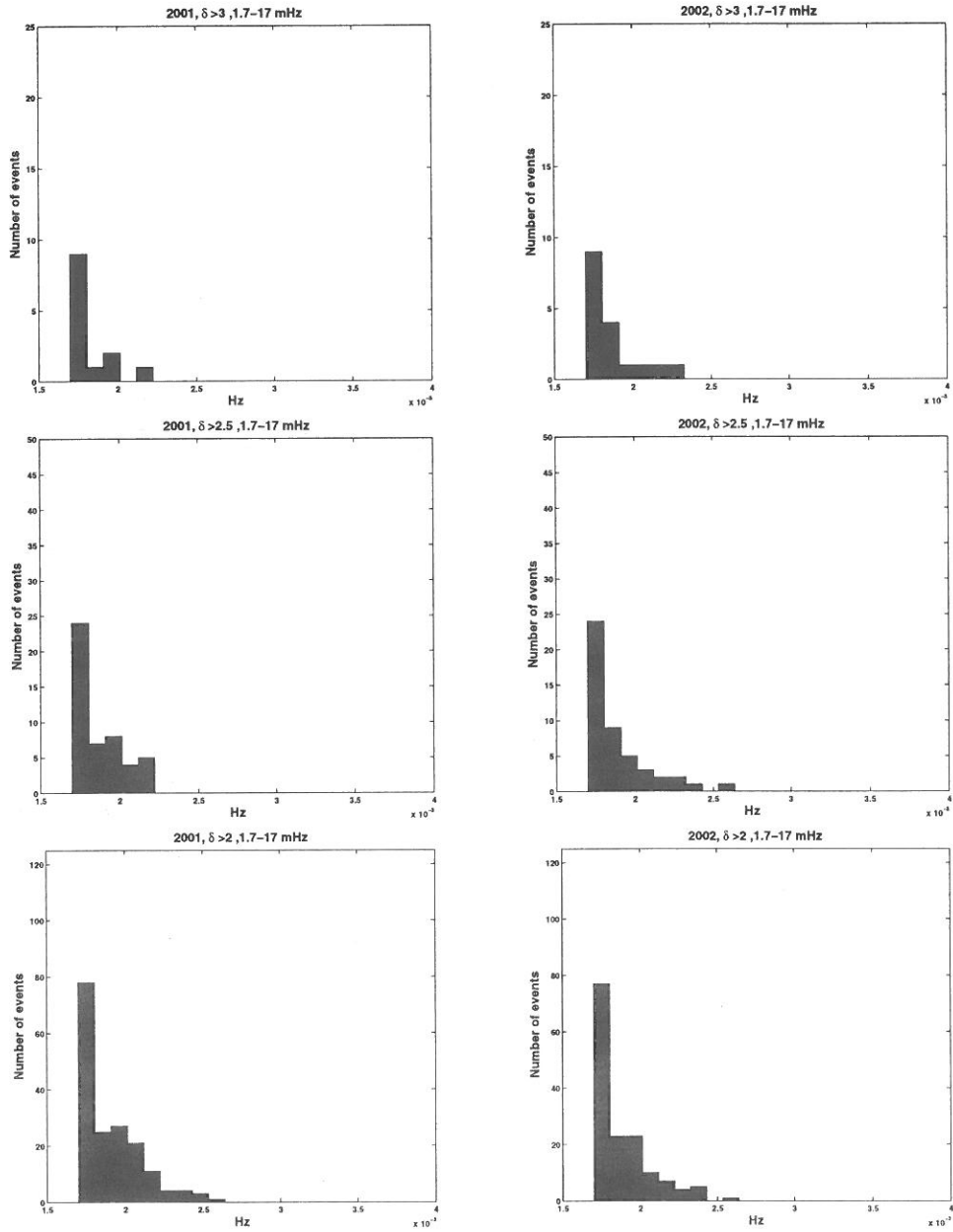Figure 18: Frequency distribution of the events during 1999 and 2000.

46
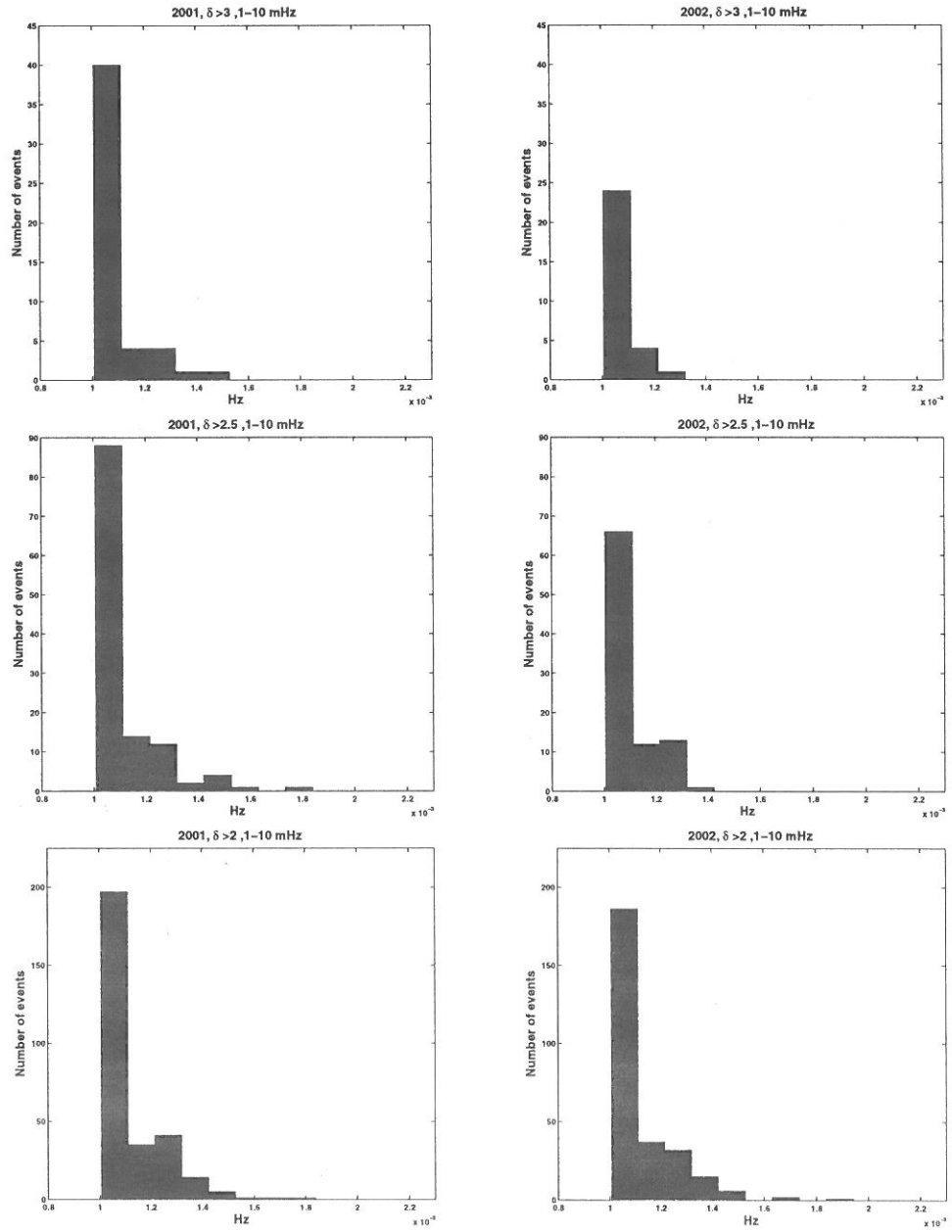
Figure 19: Frequency distribution of the events during 2001 and 2002.
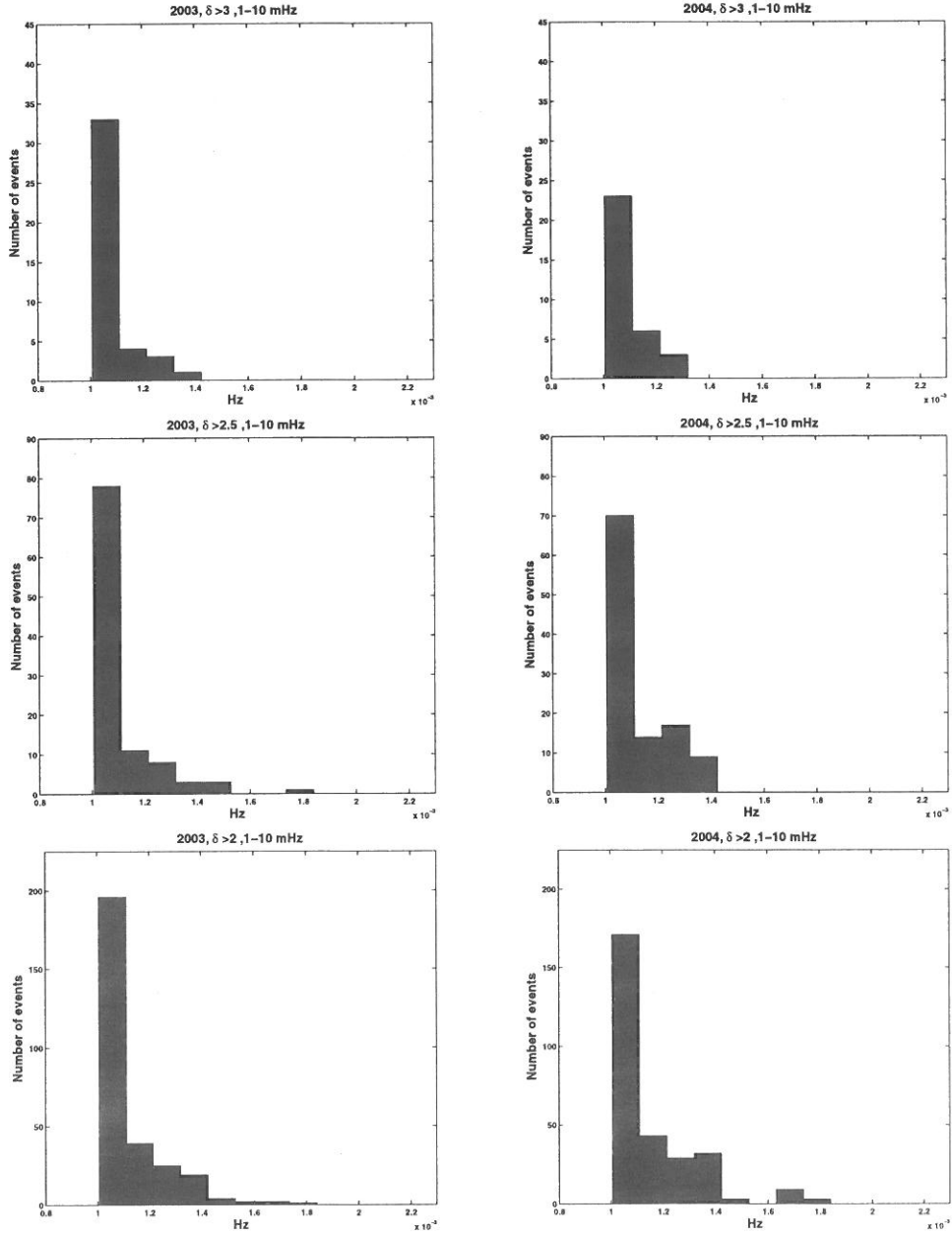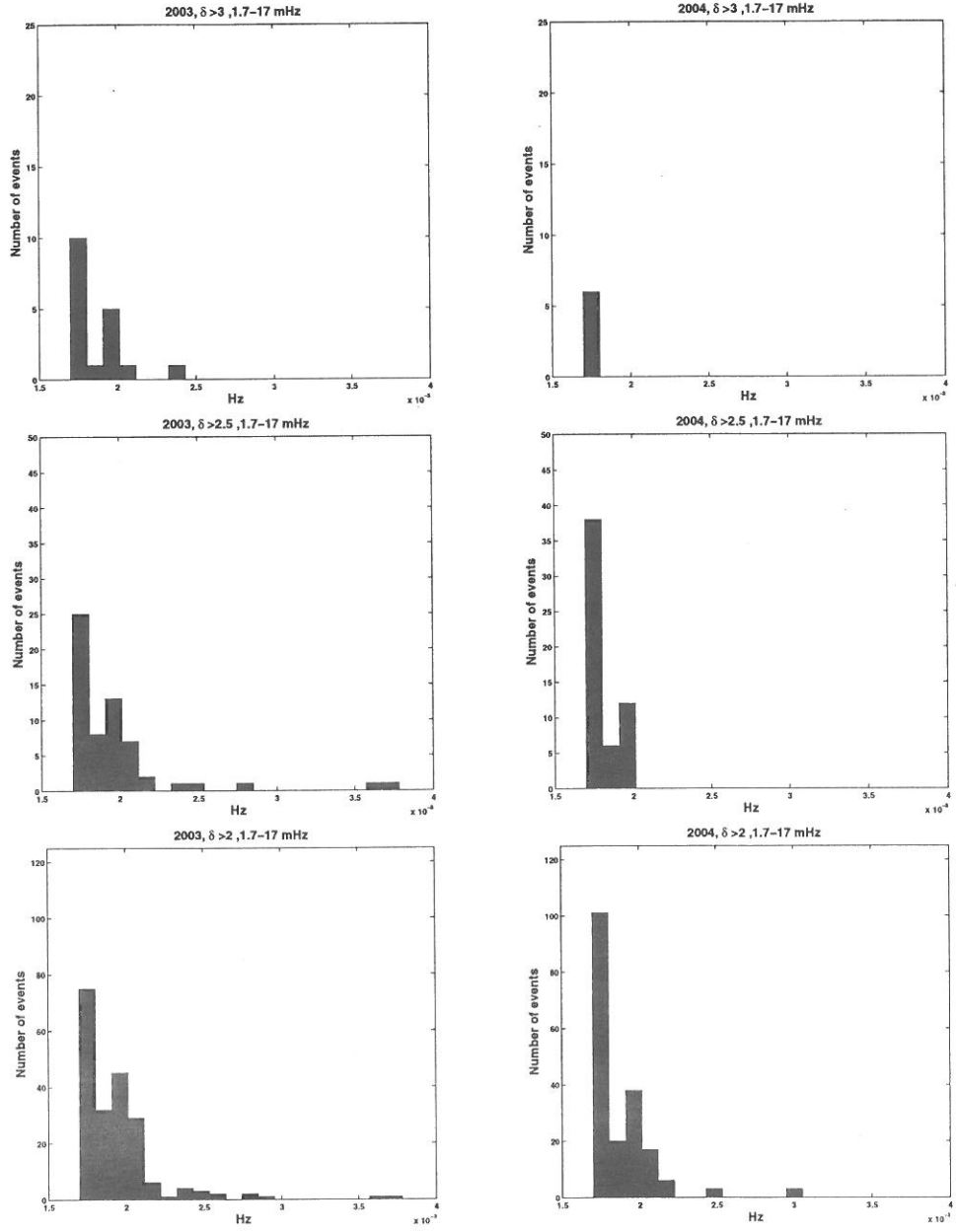
Figure 20: Frequency distribution of the events during 2003 and 2004.

Higher Frequency span (1.7-17.0 mHz) - one-peak analysis

In the figure below frequency distribution diagrams for 1997-2004 for UFS for all the different settings on δ are shown.

The yearly frequency distributions for this one-peak analysis can be found in the following pages in this Appendix.
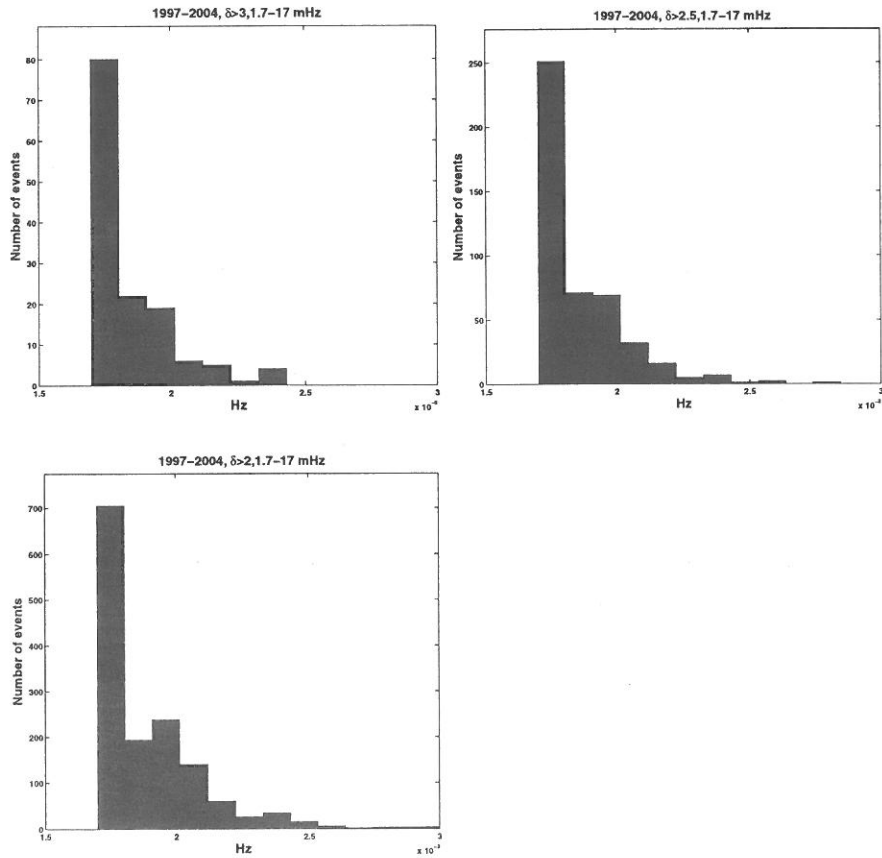
Figure 21: Frequency distribution for the events during 1997-2004 for the higher frequency span (UFS) and for the one-peak analysis.

Figure 22: Frequency distribution of the events during 1997 and 1998.

Figure 23: Frequency distribution of the events during 1999 and 2000.

Figure 24: Frequency distribution of the events during 2001 and 2002.

Figure 25: Frequency distribution of the events during 2003 and 2004.

C. Angular distribution of the mean magnetic field

The angle of the total magnetic field during the events was calculated using the 6 hour mean values of the the magnetic field components. Figure 26 shows the total angular distribution for the years covered in this study (1997-2004). The following pages show the yearly angular distribution for the investigated frequency spans. The analysis has also been made for spectra which show two peaks but only the figures for the one-peak analysis is shown. This is done because it is difficult to see any difference between the two analyses with respect to the direction of the total magnetic field. In addition, the two-peak analysis show many fewer events and is thus related to larger uncertainty.
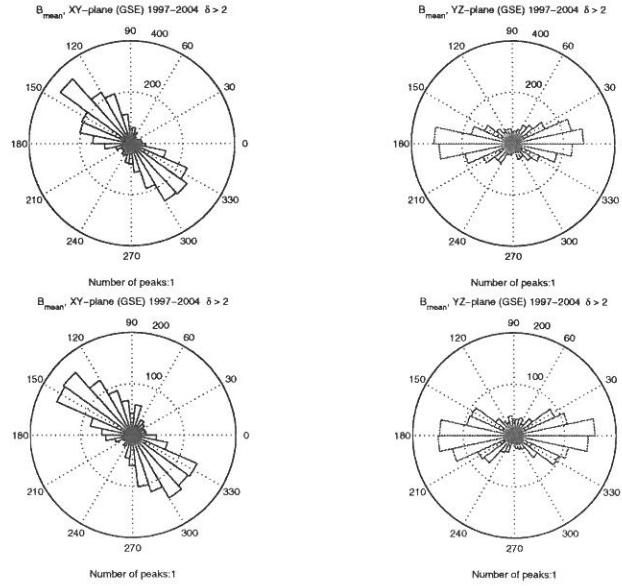

Figure 26: The top diagram shows the angular distribution in the XY-plane (left) and the YZ-plane (right) for the lower frequency span of 1-10 mHz. The bottom diagram is the corresponding analysis for the higher frequency span of 1.7-17.0 mHz. 0 degrees in the YZ-diagram corresponds to a northward directed magnetic field. The XY-diagram should be imagined as the ecliptic plane where the Sun is to the left and the Earth is to the right.
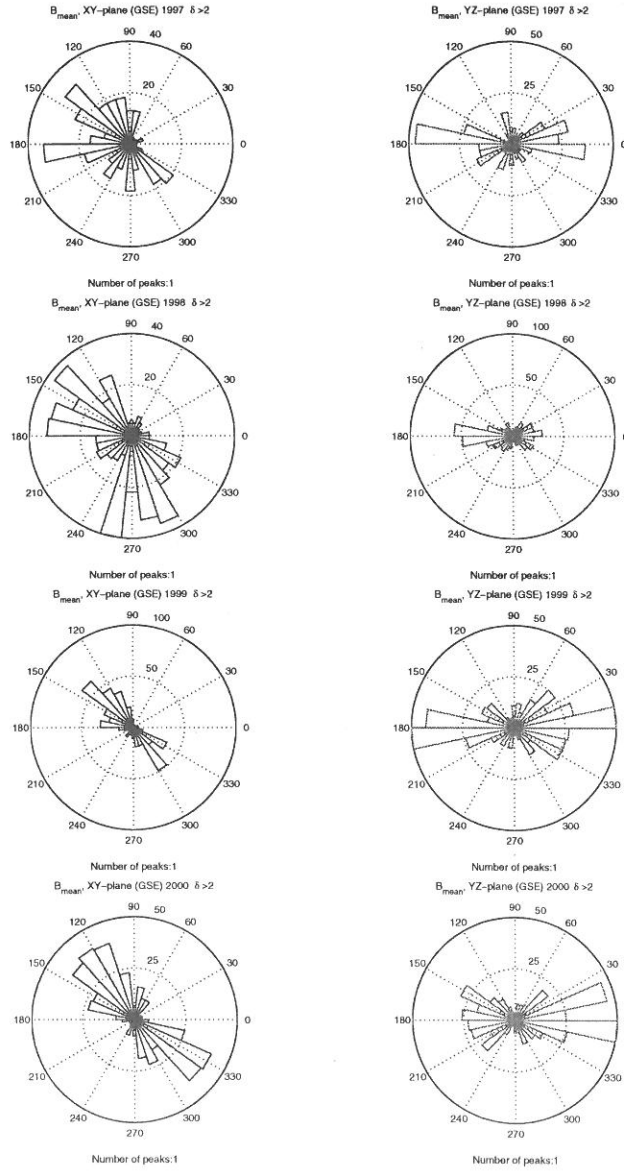
Figure 27: The yearly angular distribution for 1997 to 2000 for the lower frequency span 1-10 mHz.
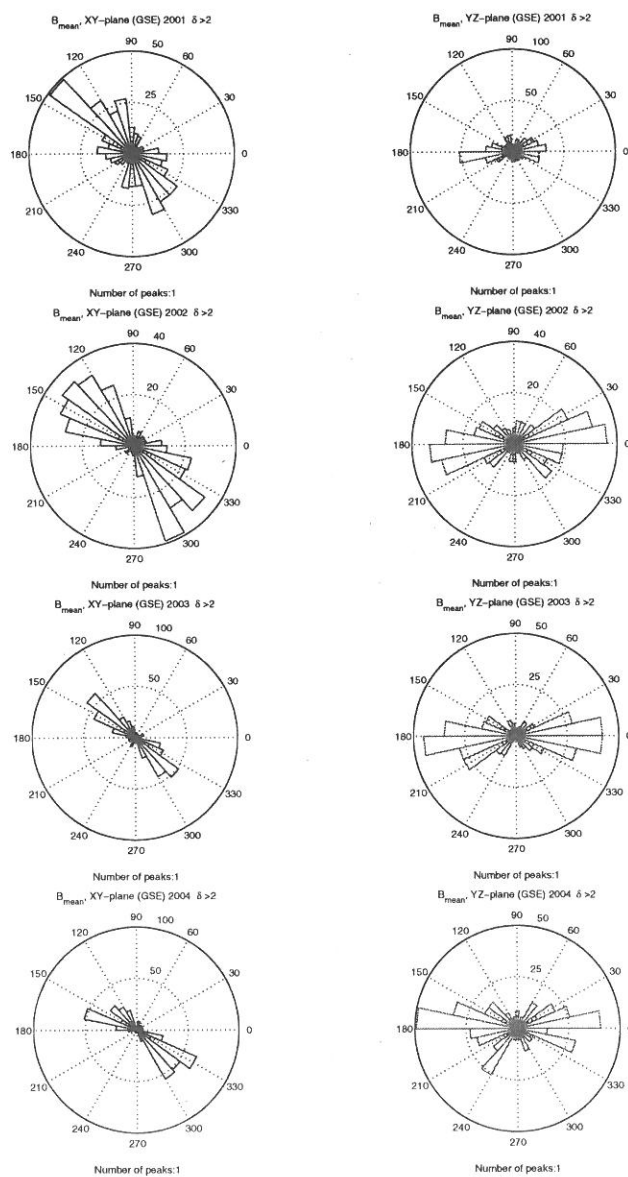
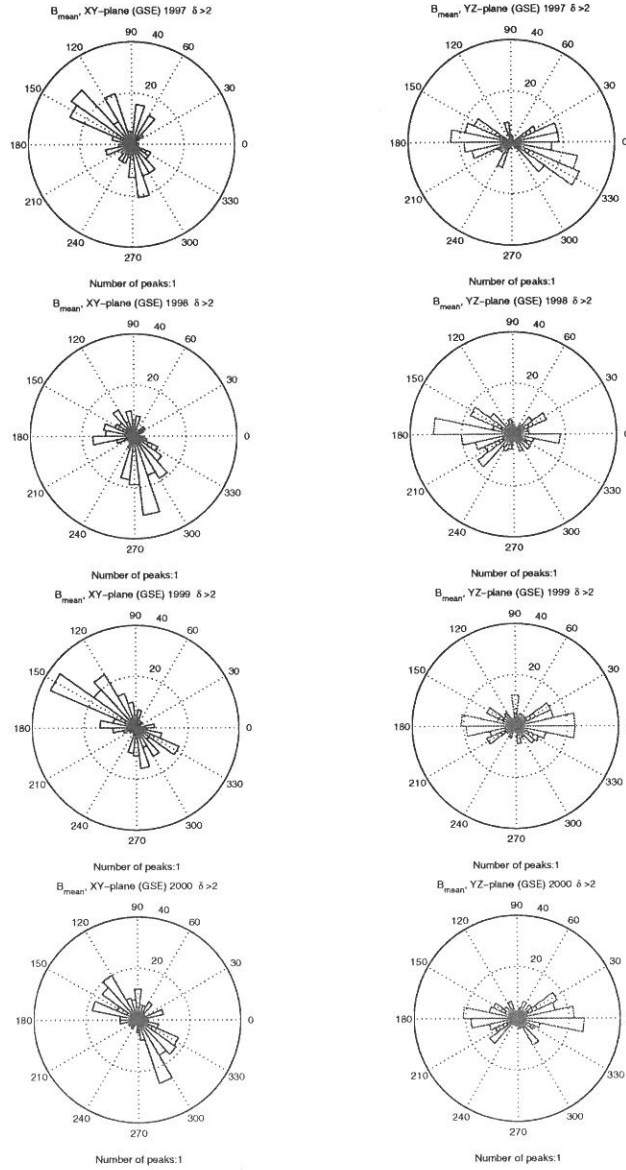Figure 28: The yearly angular distribution for 2001 to 2004 for the lower frequency span 1-10 mHz.

Figure 29: The yearly angular distribution for 1997 to 2000 for the higher frequency span 1.7-17.0 mHz.
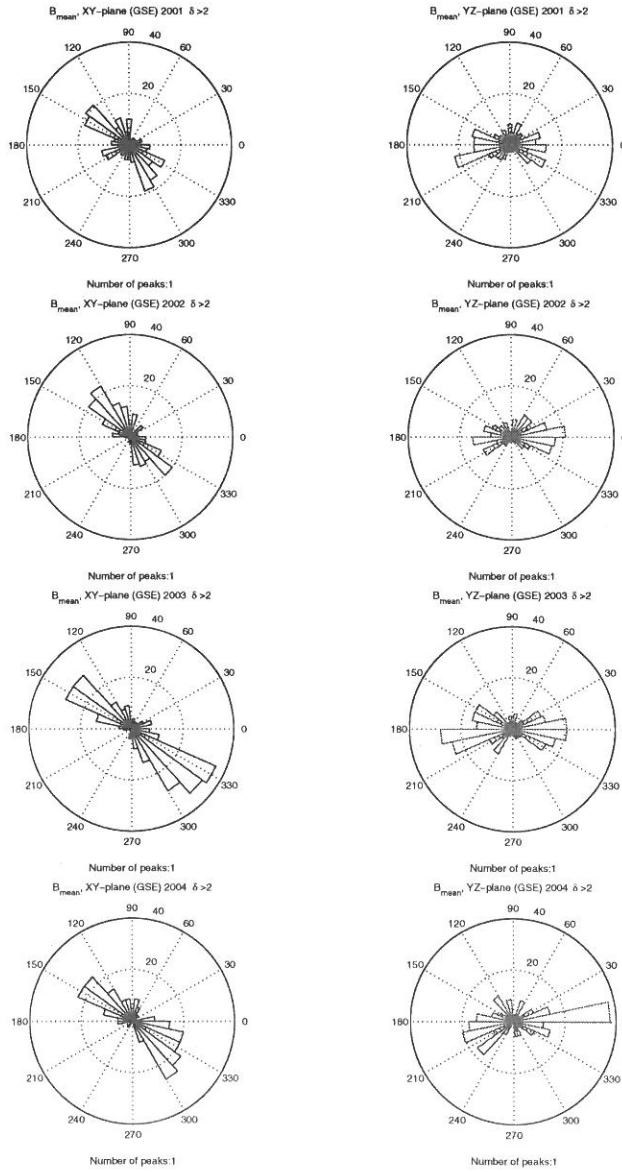
Figure 30: The yearly angular distribution for 2001 to 2004 for the higher frequency span 1.7-17.0 mHz